https://doi.org/10.5194/egusphere-2025-571
Preprint. Discussion started: 17 February 2025

An Atlantic wide assessment of marine heatwaves beyond the surface in an eddy-rich ocean model

Tobias Schulzki[1], Franziska U. Schwarzkopf[1], and Arne Biastoch[1,2]

[1]GEOMAR Helmholtz Center for Ocean Research, Kiel, Germany
[2]Christian-Albrechts Universität zu Kiel, Kiel, Germany

Correspondence: Tobias Schulzki (tschulzki@geomar.de)

Abstract. Periods of prolonged anomalously high temperatures in the ocean, known as marine heatwaves (MHWs), can have devastating effects on ecosystems. While MHWs are extensively studied in the near-surface ocean, little is known about MHWs at depth. As continuous observations in space and time are very sparse away from the surface, basin wide studies on MHWs at depth have to rely on models. This introduces additional challenges due to the long adjustment timescale of the deep ocean, resulting in a long-term drift following the model's initialisation. This unrealistic model drift dominates the MHW statistics below approximately 100 m when a fixed baseline is used. As a result, MHW studies at depth require a long model spin-up, or have to apply a linear baseline removing temperature trends. Based on a comparison of two model configurations with eddy-permitting and eddy-rich horizontal resolution, we show that the representation of mesoscale dynamics leads to pronounced differences in the characteristics of MHWs, in particular along the boundaries and along pathways of highly variable currents. Our results highlight the importance of horizontal and vertical heat transport within the ocean on sub-surface, but also on near-surface, MHWs. By investigating the vertical coherence of MHWs in an example region, here the Cape Verde archipelago, we show that MHWs are coherent over layers of a few 100 to 1000 m thickness, independent of the baseline used. These ranges are closely related to the vertical structure of the temperature field.

1 Introduction

Marine heatwaves (MHWs) are defined as prolonged periods of anomalously high temperature in the ocean (Hobday et al., 2016). As they can have devastating impacts on marine ecosystems they became a major focus of research over the last decade (Smale et al., 2019; Smith et al., 2023). Several recent studies have shown that MHWs are also connected to a range of physical impacts. Berthou et al. (2024) for example connected the 2023 MHW in the eastern Atlantic to higher land temperatures and increased precipitation probability in the UK and Radfar et al. (2024) showed that MHWs can influence the development of hurricanes. Furthermore, the study of Krüger et al. (2023) suggests that anomalously high ocean temperatures in the North Atlantic might reduce atmospheric heatwaves in Europe, even though they did not explicitly study the impact of MHWs.

https://doi.org/10.5194/egusphere-2025-571
Preprint. Discussion started: 17 February 2025

A variety of studies exist analysing the characteristics and changes of MHWs at the surface from model and observation based datasets, but there is still limited knowledge about MHWs at depth. Recently a number of studies were published that aim to understand the occurrence of MHWs beyond the surface, but mostly with a regional focus and typically considering the upper few 100 meters only (Großelindemann et al., 2022; Behrens et al., 2019; Sun et al., 2023; Amaya et al., 2023a; Zhang et al., 2023; Schaeffer and Roughan, 2017; Elzahaby and Schaeffer, 2019). Fragkopoulou et al. (2023) used a global ocean reanalysis to study characteristics of MHWs at a limited number of depth levels reaching beyond 2000 m. These studies generally agree on MHWs below the mixed layer having very different characteristics from surface MHWs. Therefore, it is not possible to make statements about deep MHWs based on the sea surface temperature. As a consequence, in vast areas of the ocean the characteristics and drivers of MHWs beyond the surface have not been identified. Although the surface heat flux is undoubtedly important for surface MHWs in many regions (e.g. Holbrook et al., 2019), Großelindemann et al. (2022); Behrens et al. (2019); Elzahaby et al. (2021); Gawarkiewicz et al. (2019); Chen et al. (2022) and Wu and He (2024) highlight the importance of ocean currents and mesoscale features for generating (sub-)surface MHWs. Further, Hövel et al. (2022); Goes et al. (2024) demonstrate that changes in ocean advection can modulate interannual to decadal variability of the MHW frequency and result in a potential source of predictability. Vertical heat transports and mixing within the ocean are also considered important to generate MHWs themselves, or to set the vertical extend of surface forced MHWs (Schaeffer and Roughan, 2017; Chen et al., 2022).Vertical velocities in the ocean typically show much stronger spatial variations than the surface heat flux and could thus lead to a decoupling of surface and sub-surface MHWs. The importance of ocean dynamics is likely even more important in the deep compared to the near-surface ocean, but a comprehensive analysis of MHWs throughout the entire water column is currently missing. This especially includes MHWs that occur along the seafloor, which provides a unique habitat for various marine species, such as sponges and corals. These ecosystems exist in shallow seas, but also deep ocean areas (Roberts et al., 2006; Maldonado et al., 2017) and may be vulnerable to MHWs (Marzinelli et al., 2015; Short et al., 2015; Wyatt et al., 2023; Wu and He, 2024).

Since direct temperature measurements are rare beyond the typical depth of ARGO floats (1000 m) and in particular close to bathymetric features, basin wide assessments of MHWs at depth must rely on ocean models, which comes with several challenges.

MHWs are commonly defined as prolonged periods of anomalously high temperature above a seasonally varying baseline (Hobday et al., 2016). Nevertheless, differences exist in the methodology used to define this baseline and the corresponding threshold that must be exceeded in order to identify a temperature anomaly as a MHW. Most studies use a 30-year long baseline period that can be placed in the beginning or end of the available timeseries, if it is longer than 30-years (e.g. Guo et al., 2022). For shorter timeseries the full available timeseries is typically used (e.g. Fragkopoulou et al., 2023), but also for longer timeseries the full timeseries may be used (e.g. Großelindemann et al., 2022). A strong debate evolved around the question whether the baseline should be fixed for a historic reference period, or evolve with a globally rising temperature (Oliver et al., 2021; Amaya et al., 2023b). This question is frequently discussed in the context of future projections, but already over the historic period trends in surface temperature strongly change the characteristics of MHWs over time (Chiswell, 2022).

https://doi.org/10.5194/egusphere-2025-571
Preprint. Discussion started: 17 February 2025

The debate focuses on the interpretation of the results and in general all these approaches yield meaningful results. However, the choice of the baseline becomes even more important for models that often do not just simulate real trends that are tied to the surface forcing or changes in circulation, but also low frequency adjustments to the initial conditions known as 'model drift' (e.g. Tsujino et al., 2020). Such a model drift only occurs in the model and has no real world counterpart. Since the near-surface ocean typically adjusts much faster than the deep ocean, model drift becomes increasingly important when MHWs are to be studied at mid- and abyssal depths. As a consequence, the impact of model drift has not gained a lot of attention in the surface focused MHW literature, but will be examined here in detail.

Other important questions arise when performing a basin wide assessment of MHWs in models. Hobday et al. (2016) mention that the statistics of MHWs are likely dependent on the temporal and spatial resolution of the dataset. Regarding the temporal resolution, nearly all studies use daily mean records following Hobday et al. (2016). The impact of horizontal resolution is less clear. When interpolating a high-resolution temperature dataset on a coarse grid, local temperature anomalies are reduced, but also variability is reduced. It is not obvious whether these concurring effects cancel out, or if they lead to more/less MHWs that are detected on a coarser grid. As a consequence, it is not clear whether MHWs detected on the native grid of different model and observation based datasets are directly comparable.

In models another layer of complexity is added by the resolution of the model itself. Model resolution strongly changes local temperature variability (e.g. through the presence of eddies), but also large-scale dynamics (more realistic current strength, pathways and variability). This could directly translate into changes of MHW statistics, as eddies were shown to drive MHWs (Großelindemann et al., 2022; Elzahaby and Schaeffer, 2019; Wyatt et al., 2023; Wu and He, 2024) and MHWs at depth occur most frequently along the pathways of deep currents (Fragkopoulou et al., 2023).

Overall, there remains a lack of knowledge regarding MHWs in the deep ocean and critical challenges in detecting them within models. The overarching goal of this study is to provide a manageable dataset suited for comprehensive studies of MHWs and their impacts throughout the entire Atlantic ocean, in particular including the deep ocean. We use a hierarchy of grids to study the impact of dataset and model resolution on the derived MHW statistics. Further, we study the suitability of different baselines to define MHWs at depth, given the added complexity of model drift after initialisation. We aim to provide a detailed evaluation of different MHW detection methodologies when applied to depth levels away from the surface that may be useful for many following studies. At the same time, we investigate the impact of mesoscale dynamics, ocean currents as well as surface forced and model related trends on the occurrence and characteristics of MHWs throughout the entire Atlantic Ocean, including MHWs at the seafloor. In a last step we investigate which processes determine the vertical coherence of MHWs in more detail for a selected region. Here the Cape Verde archipelago in the eastern subtropical Atlantic is chosen as an example, due to its high biological productivity and ecosystems covering a large depth range in a horizontally confined region.

https://doi.org/10.5194/egusphere-2025-571
Preprint. Discussion started: 17 February 2025

2 Data and Methods

2.1 Model simulations

This study and the resulting dataset of MHWs is based on simulations in VIKING20X (described in detail by Biastoch et al., 2021), an ocean/sea-ice model configuration employing the NEMO code (version 3.6, Madec, 2016) with its two-way nesting capability AGRIF (Debreu et al., 2008), covering the Atlantic ocean at 1/20° horizontal resolution and 46 vertical z-levels. The bottom-topography is represented by partial steps (Barnier et al., 2006). The two-way nature of the nesting approach not only provides lateral boundary conditions from the hosting global coarse (1/4°) resolution grid (hereafter referred to as host grid) to the high resolution nest, but also frequently updates the former with the solution on the nest grid by interpolation. For tracer variables, such as temperature, the solution on the host grid within the nested area represents a coarsened version of the nest solution. It therefore includes the dynamical impacts of the higher resolution.

Following the OMIP-II protocol (Tsujino et al., 2020) a series of six consecutive hindcast simulations from 1958 to 2019 forced by the JRA55-do atmospheric dataset (Tsujino et al., 2018) have been performed of which the first cycle (referred to as VIKING20X-JRA-OMIP in Biastoch et al., 2021) has been initialized from hydrographic data provided by the World Ocean Atlas 2013 (WOA13; Locarnini et al., 2013; Zweng et al., 2013) and an ocean at rest, while each following cycle has been initialised from the ocean state at the end of the preceding one. While the transition between the cycles is always between 2019 and 1958, each individual cycle has been extended until 2023. From this series, only the first and sixth cycles for the period 1980-2022 are analysed in this study.

VIKING20X was successfully used in various studies, proving the models capability to realistically simulate the large-scale circulation and its variability (Biastoch et al., 2021; Böning et al., 2023; Rühs et al., 2021), as well as the regional circulation in many locations from the surface to the deep ocean (Fox et al., 2022; Schulzki et al., 2024). Furthermore, the model proved highly capable in simulating MHWs on the Northeast U.S. continental shelf (Großelindemann et al., 2022).

A parallel series of simulations has been performed in ORCA025, the hosting configuration of VIKING20X at 1/4° horizontal resolution, following the same strategy (the first two cycles are referred to as ORCA025-JRA-OMIP(-2nd) and described in detail in Biastoch et al., 2021). Here the period 1980-2022 of only the sixth cycle is used. The two hindcast series in VIKING20X and ORCA025 are directly comparable, with the only difference being the increased resolution in the Atlantic Ocean in VIKING20X.

2.2 Definition of marine heatwaves

Marine heatwaves are defined based on the definition of Hobday et al. (2016). For each day of the year the climatological mean and 90th percentile of all temperature values within a 11-day window are estimated. Afterwards they are smoothed using a 31-day moving average. MHWs were detected using the xmhw python package (Petrelli, 2023). A MHW occurs, if the temperature exceeds the seasonally varying 90th percentile for at least 5 days. If the gap between two MHWs is not longer than 2 days, they are considered as a single event.

https://doi.org/10.5194/egusphere-2025-571
Preprint. Discussion started: 17 February 2025

MHWs are defined locally, meaning the definition is applied at each individual grid point without considering information from other grid points. As a result, the definition can be applied to all depth levels without any modification even though temperature variability is typically much weaker in the deep ocean than it is at the surface.

Although most studies apply the Hobday et al. (2016) definition, a variety of different temperature baselines are used to define MHWs. We apply 3 of the most commonly used baselines in this study. First, a fixed threshold where the climatology is calculated for the whole time period analysed here (1980-2022). Second, we apply a fixed 30-year baseline that follows the latest period used to define the World Meteorological Organisation (WMO) climate normals (1991-2020; WMO-No.1203, 2017). The third baseline used is a linearly increasing baseline. Here temperature anomalies are defined relative to the linear trend based on the time period 1980-2022. This is achieved by detrending the temperature timeseries at each grid point before calculating the climatology and performing the MHW detection. A non-linear threshold following Chiswell (2022) was also tested, but is only briefly mentioned in the following results. We acknowledge that various other definitions of the baseline were applied in previous studies, linked to different scientific questions and motivations. Nevertheless, our results can often be transferred to other baselines as well, even if their exact definition may slightly differ from the ones used here.

Annual mean timeseries of frequency, duration and intensity are created by averaging all events that started in a specific year. For the event based characteristics, namely duration and maximum intensity, spatial averages are calculated without taking grid cells into account where no MHWs occur. For the area based characteristics, namely the number of MHWs and number of MHW days that occur in a region, grid cells without MHWs are included in the calculation.

2.3 Choice of the horizontal grid

The host grid of VIKING20X represents a coarsened version of the nest temperature that contains mesoscale dynamics (see descripton of the two-way nesting technique above). In order to assess whether the derived MHW statistics are sensitive to the resolution of the temperature dataset, we compare MHWs detected on the VIKING20X nest grid and the coarser host grid. In both cases we only derive statistics in the Atlantic that is covered by both, the nest and the host grids. Here we only show results using a linear baseline, but the conclusions of this section do not change when other baselines are used.

Statistics for the whole Atlantic do not differ between the coarser host grid and the high-resolution nest grid. This is true for all depth levels, including the ones shown in figure 1a-c.

The horizontal patterns are not dependent on the dataset resolution either (figure 1d,e). Although the grid is coarser as apparent by individual pixels, the patterns are almost the same. The reason for this result is that MHWs do not occur at a single nest grid point. The zonal and meridional de-correlation scales of the daily temperature timeseries (with the mean seasonal cycle removed) are larger than 0.3° even in highly variable regions such as the Gulf Stream separation (not shown) and thus larger than the target grid size (1/4°). As a result, interpolation from the 1/20° to the 1/4° grid does not impact the derived MHW statistics. For interpolation onto an even coarser grid differences are expected in certain regions.

To detect MHWs along the coasts, the higher resolution dataset is advantageous due to the more realistic coastline itself. Otherwise, results are still similar along the ocean boundaries (figure 1d,e). The same argument holds for the seafloor, which

https://doi.org/10.5194/egusphere-2025-571
Preprint. Discussion started: 17 February 2025

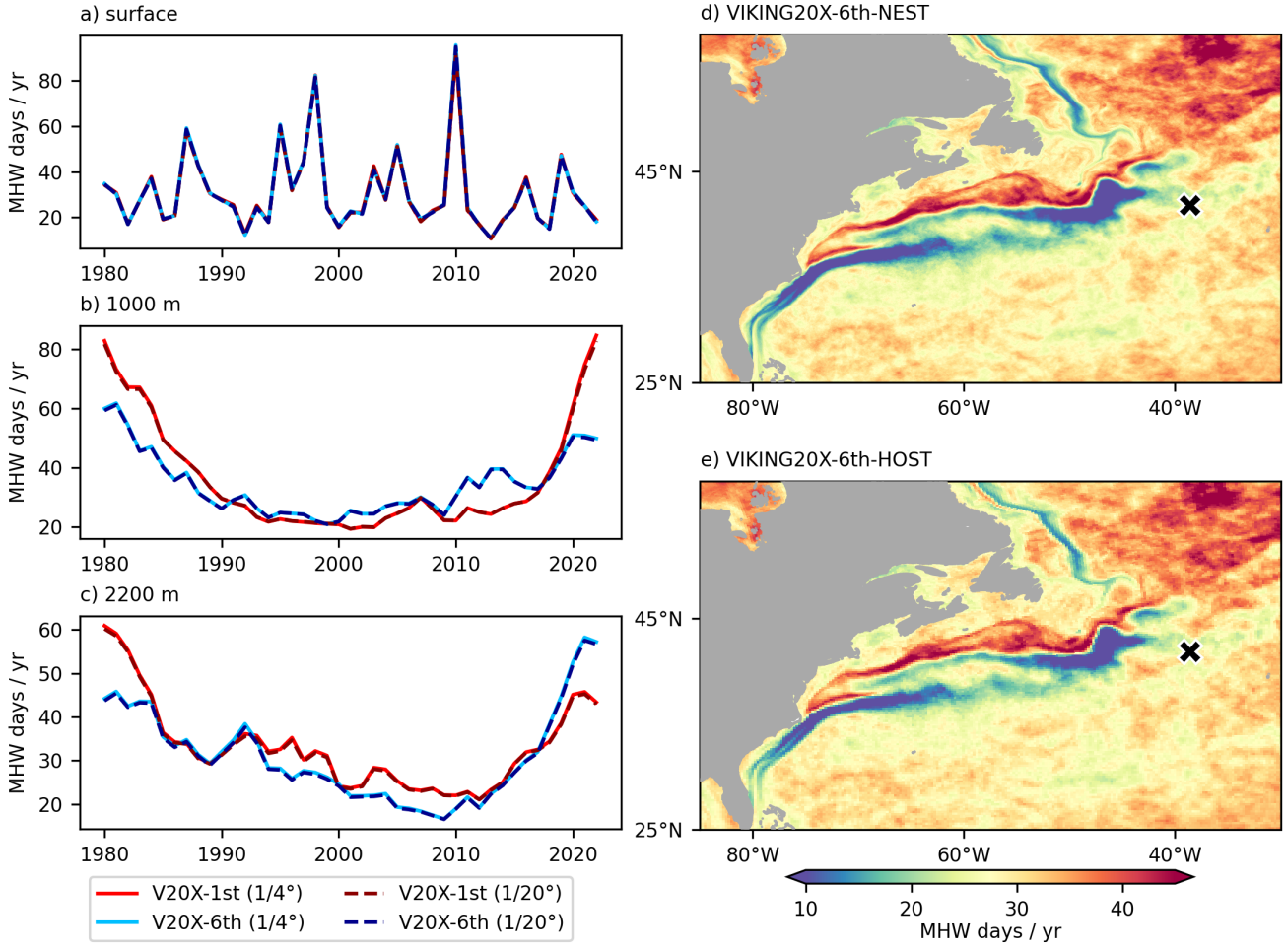

Figure 1. Number of MHW days per year in different depths, derived from the nest (1/20°) and coarse host (1/4°) grids (Atlantic only) of the first and sixth cycles in VIKING20X (V20X-1st and -6th). Maps show the mean (1980-2022) number of MHW days per year at the surface derived on the nest and host grids (6th cycle). The cross indicates the grid point used as an example in figure 2.

is more realistically represented at higher horizontal resolution. Statistics for larger domains can be calculated on the coarser grid, which significantly decreases the computational costs of detecting MHWs. Accordingly, the following analysis, except for the analysis of bottom MHWs, is carried out on the global host grid of VIKING20X only.

2.4 Heat budget

In order to study the vertical coherence of MHWs in detail, we calculate the heat budget for an example region, here the Cape Verde archipelago in the eastern subtropical Atlantic. The heat content of a given depth level $OHC(z)$ [in J] is calculated from:

https://doi.org/10.5194/egusphere-2025-571
Preprint. Discussion started: 17 February 2025

$$OHC(z) = \rho_0 c_p \int_A T \triangle z dA \tag{1}$$

Here A is the area of the Cape Verde archipelago (26°W-22°W, 13.9°N-18.7°N, see figure 8) and T the temperature. The temperature is provided in $°C$, or equivalently we use a reference temperature of 273.15 K. $\triangle z$ is the grid cell thickness. $\rho_0 = 1026\ kg\ m^{-3}$ and $c_p = 3991.87 J\ kg^{-1}\ K^{-1}$ are the reference density and specific heat capacity. The values are taken from the NEMO routine that is used to calculate the surface heat flux.

The surface heat flux itself is stored in the NEMO ocean model output and integrated over the same area A.

The ocean heat transport across all sections bounding the area A within a given depth layer $OHT(z)$ [in W] is calculated from:

$$OHT(z) = \rho_0 c_p \int_L u_\perp T \triangle z dL \tag{2}$$

Here $u_\perp$ is the velocity perpendicular to the section. L is a 2D section and dL is the length of a section segment.

Similarly, the vertical heat transport $Vert(z)$ [in W] is calculated from:

$$Vert(z) = \rho_0 c_p \int_A w T dA \tag{3}$$

where w is the vertical velocity.

As we are interested in anomalies relative to the mean seasonal cycle (see MHW definition), the seasonal cycle is removed for all heat budget terms.

To investigate the heat budget in certain depth ranges, we sum up the terms vertically. The residual between ocean heat content change and net horizontal and vertical heat transport (which includes the surface heat flux if the upper boundary is the ocean's surface) represents all heat budget terms that are missing from the calculations described above. This includes horizontal diffusion across the lateral boundaries, but more important vertical mixing.

3 Results

3.1 Impact of long-term trends on MHW statistics

While the choice of the baseline is important for the interpretation of MHWs at the surface from observations, it is even more important in models. Most models do not just contain 'real' trends related to the surface forcing, or changes in circulation, but also trends that arise from an adjustment of the model after initialisation ('model drift'; see for example Tsujino et al., 2020). This model drift can have a different magnitude and sign at different depth levels (figure 2). While in the top 100 m the model adjusts fast and for the period 1980-2022 trends are similar in the 1st and 6th cycle, major differences between the cycles occur

https://doi.org/10.5194/egusphere-2025-571
Preprint. Discussion started: 17 February 2025

at greater depth. Around 1000 m the ocean shows a strong cooling trend in the 1st cycle, while it warms in the 6th cycle. At 2200 m the ocean warms in the 1st cycle, while it slightly cools in the 6th.

The impact of different baseline definitions on the occurrence of MHWs in the presence and absence of model drift is illustrated in figure 2c-h. A location in the deep (2200 m) subtropical North Atlantic is used as an example here. The temperature in the 1st cycle shows pronounced multi-decadal variability with high temperatures during the first and last 10 years of the timeseries and lower temperatures in between. In the presence of strong model drift (1st cycle) multidecadal variability is only captured by the MHW statistics when a linear baseline is used. With all other baselines a linear trend in the temperature leads to MHWs only occurring in the later period. This is different in the 6th cycle, where, without a linear temperature trend, the different baselines yield more similar results. Also, for the linear baseline the results are more similar between the two cycles. While the correlation between the timeseries of the 1st and 6th cycle is higher than 0.9 at the surface and in 100 m for all baselines, there is a weak anti correlation (about -0.3) in 1000 m and 2200 m for the WMO and fixed baselines. The linear baseline timeseries are still highly correlated between the 1st and 6th cycles in 1000 m (0.91) and in 2200 m (0.85).

On the one hand this, suggests that the MHWs derived at this particular location in the 1st cycle are dominated by unrealistic drift, except when a linear baseline is used. On the other hand, it suggests the linear temperature trend over the last 40-years was of minor importance. Instead changes in the occurrence and characteristics of MHWs were dominated by (multi-)decadal variability, independent of the baseline used for detection.

The impact of model drift in temperature is directly reflected in the basin wide MHW statistics as well. At the surface and in 100 m depth MHW statistics are robust across the cycles (figure 3a,b), suggesting that the trend is mostly caused by the common surface forcing. In contrast, a strong drift in the temperature of the 1st cycle leads to major differences at depth, if the fixed and WMO baselines are applied. At 1000 m depth, the number of MHW days is small before and increases after 2000 in the 6th cycle, but shows a sharp decline in the 1980s and then stays near zero in the 1st cycle. At 2200m the ocean reaches a near-permanent MHW state toward the end of the timeseries (365 MHW days per year). The strong increase in MHW days is more pronounced with the WMO baseline. This is because the threshold at 2200 m is lower when the first 10 years are not included, since the mid-depth ocean was warmer in the 80s than in the 90s in most regions (see figure 2 as an example). In contrast, the 6th cycle shows a decrease in MHW days from around 100 to almost no MHW days per year until the 1990s.

Using a linear baseline (detrending) removes most of the model drift, but it also removes any forcing related trends. This is particularly visible at the surface and in 100 m depth. Therefore, it is not possible to recover the MHW statistics from non-detrended temperatures in the 6th cycle by detrending the 1st cycle (e.g. 1st-linear does not match 6th-fixed/WMO). As a consequence, the 1st cycle can not be used to make any statements about the long-term evolution of MHWs relative to a fixed baseline as the evolution is dominated by the impact of model drift.

Applying the linear baseline in the 1st and 6th cycle yields more similar, but not identical, results (red lines in 3a,b). Detrending also leads to a similar evolution of the temperature itself in both cycles (e.g. figure 2e,f). This is also true for the global mean temperature at all depth levels (not shown). Therefore, assuming that model drift adds linearly to forced temperature trends is a reasonable assumption, but non-linear adjustments are not completely absent. A non-linear baseline was tested (not

https://doi.org/10.5194/egusphere-2025-571
Preprint. Discussion started: 17 February 2025

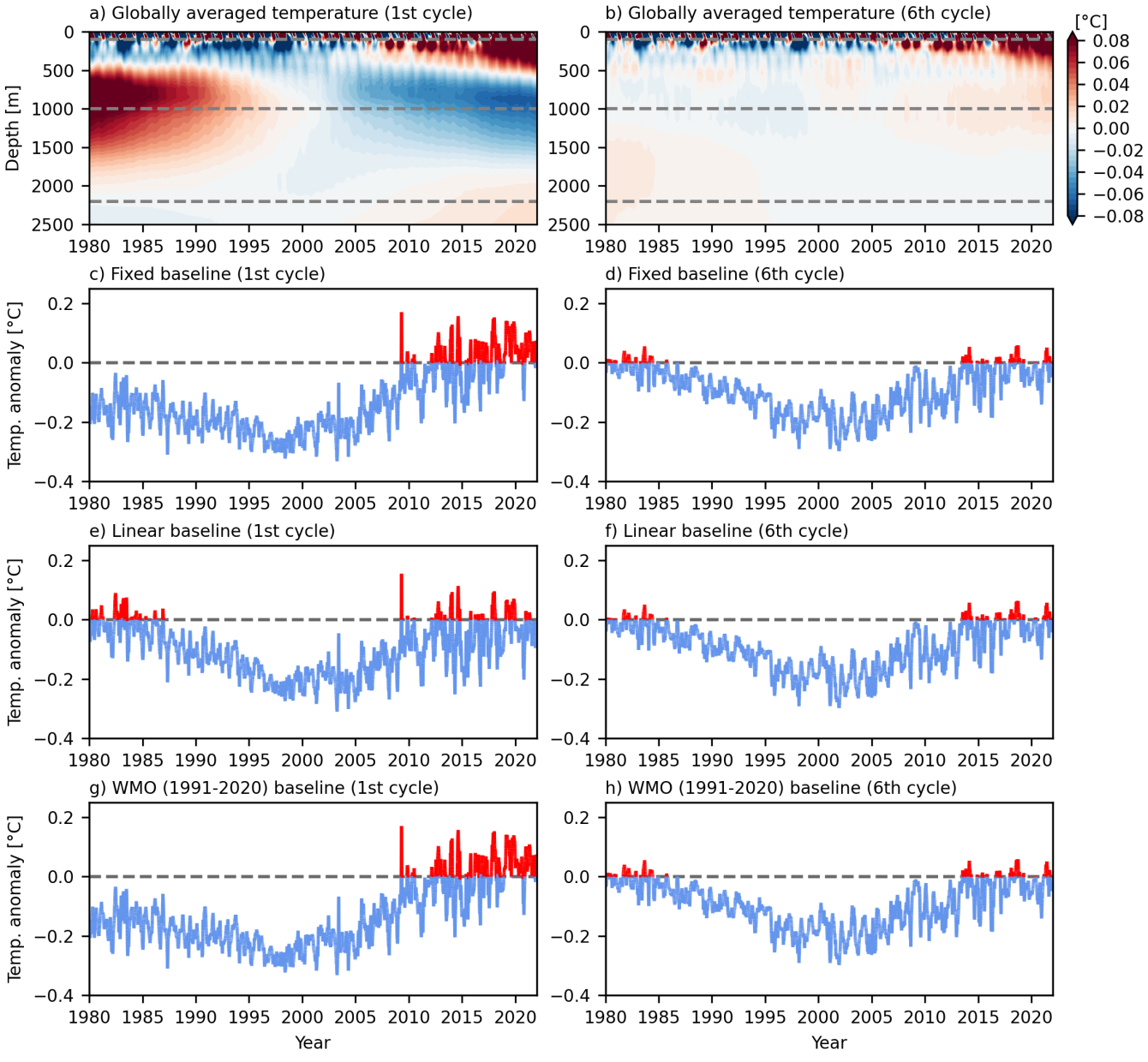

Figure 2. Globally averaged temperature anomaly relative to the 1980-2022 mean, illustrating model drift (a,b). Temperature relative to the MHW threshold estimated with different baselines at 41.8°N, 38.6°W (see cross in figure 1d,e) at 2200 m depth (c-h).

shown) as well, but yields no advantage over the linear baseline. In agreement with Chiswell (2022), differences in the derived MHW statistics are small and the non-linear baseline has disadvantages due to the finite length of the timeseries.

https://doi.org/10.5194/egusphere-2025-571
Preprint. Discussion started: 17 February 2025

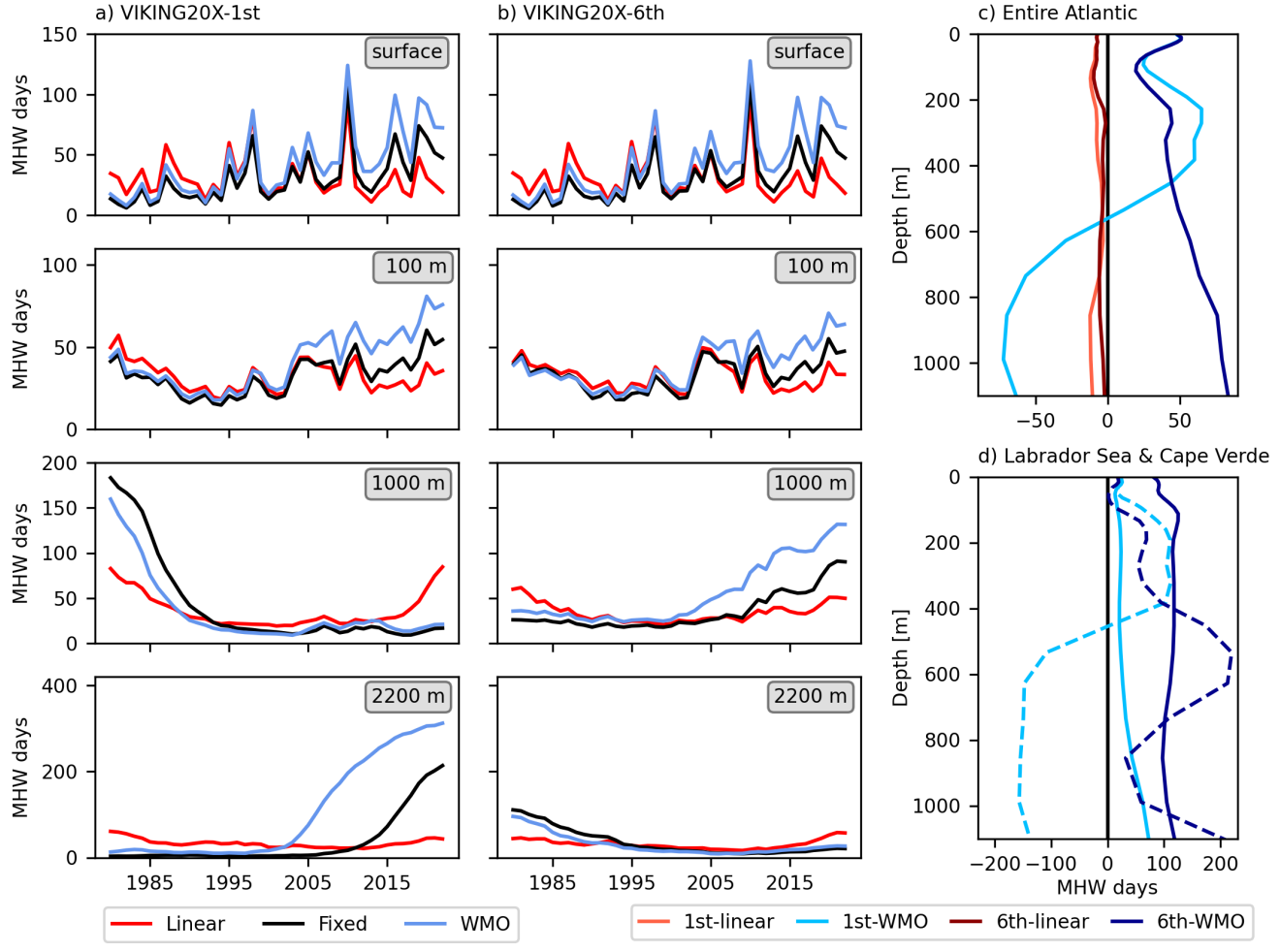

Figure 3. Number of MHW days per year averaged over the Atlantic in the 1st (a) and 6th (b) cycle at selected depths and for different baselines. Depth profiles of the difference in the number of MHW days between the last (2013-22) and first ten years (1980-89) for the entire Atlantic (c) and for the Cape Verde archipelago (d; dashed) and Labrador Sea (d; solid). For the entire Atlantic the linear and WMO baselines are shown, while in d) only results from the WMO baseline are shown.

Vertical profiles of differences between the last and first ten years of the timeseries further reveal that only in the top 100 m statistics are comparable between the 1st and 6th cycle when the WMO baseline is used (figure 3c). Below 100 m depth, the number of MHW days increases stronger in the 1st cycle from the beginning to the end of the timeseries. Below 600 m depth changes are of opposite sign in the 1st and 6th cycle.

There are regional differences, however (figure 3d). For example in the Labrador Sea (solid) results differ already at the surface. In the eastern subtropical Atlantic (Cape Verde archipelago; dashed), changes are similar within the top 50 m. This highlights that the impact of model drift is not the same everywhere. Note that the surface flux is (almost) the same in the 1st

https://doi.org/10.5194/egusphere-2025-571
Preprint. Discussion started: 17 February 2025

and 6th cycle and thus can not explain differences between the cycles. In regions where ocean advection and stratification play an important role near-surface, model drift is likely to affect the occurrence of MHWs at depths even shallower than 100 m. This is the case for the Labrador Sea, where advective processes strongly influence the mixed layer dynamics (e.g. Gelderloos et al., 2011). For the Cape Verde archipelago variability in the mixed layer, that in the annual mean extends to approximately 50 m depth, is strongly influenced by the surface heat flux as will be shown later (section 3.4).

In any case, model drift dominates long term changes in MHW statistics away from the surface. Thus, MHW detection at depths beyond approximately 100 m requires a well spun-up model, if the impact of long term trends (e.g. related to climate change) is to be studied. Model studies that focus on the surface or shallow seas are able to do so using a shorter model spin-up. With a linear baseline, statistics are not identical, but similar in the presence (1st cycle) and absence (6th cycle) of strong model drift, as the occurrence of MHWs is mostly related to interannual to decadal variability. Studies applying a linear baseline are therefore possible with a shorter model spin-up as well. In the following we focus on the characteristics of MHWs detected by applying the WMO baseline in the 6th cycle. Even though the trends of the deep ocean temperature are highly uncertain due to the lack of long-term observations, the well spun-up experiment is regarded as the best estimate available.

3.2 Horizontal and vertical changes in MHW characteristics

3.2.1 Characteristics of MHWs at the surface

Compared to the observation based NOAA OISST dataset (Huang et al., 2021), VIKING20X overestimates the duration, but underestimates the maximum intensity of MHWs at the surface (figure 4; WMO baseline). This is a well documented feature of many models compared to satellite based datasets (Qiu et al., 2021; Pilo et al., 2019). The temporal variability of the statistics are in very good agreement, however. The correlation exceeds 0.66 for all timeseries. While the magnitude of variability is similar for the frequency and maximum intensity, it is higher for the MHW duration in the model. The duration and frequency show a positive linear trend, which is slightly stronger in the NOAA OISST dataset. The maximum intensity does not show a clear trend in neither of the two datasets. The horizontal patterns of the time mean frequency and maximum intensity match the observation based product as well (note the difference in the colorbar that represents the mentioned mean bias). MHW frequency is high along the equator, in the western North Atlantic subtropical gyre and in a zonal band around 30°S. Only few MHWs per year are detected within 20° around the equator and in the eastern subpolar gyre in both, the model and observations. The Gulf Stream (GS), boundary currents of the subpolar gyre and the upwelling regions along the eastern boundary stand out with high maximum intensities. Differences between the datasets are more pronounced for the duration of MHWs. In particular between the equator and 20°N the duration is much shorter in observations. The model and observations agree on regions with longer and shorter duration in most other regions, but the difference between regions of high and low mean duration is more pronounced in the model. Differences in duration are largest in regions that show high cloud cover, especially in the Intertropical Convergence Zone (ITCZ), limiting the availability of satellite based SST. This may contribute to the larger difference in these regions compared to other parts of the Atlantic. Nevertheless, it can not be concluded that the model is more realistic and model biases (e.g. caused by limited vertical resolution) could play an important role too.

https://doi.org/10.5194/egusphere-2025-571
Preprint. Discussion started: 17 February 2025

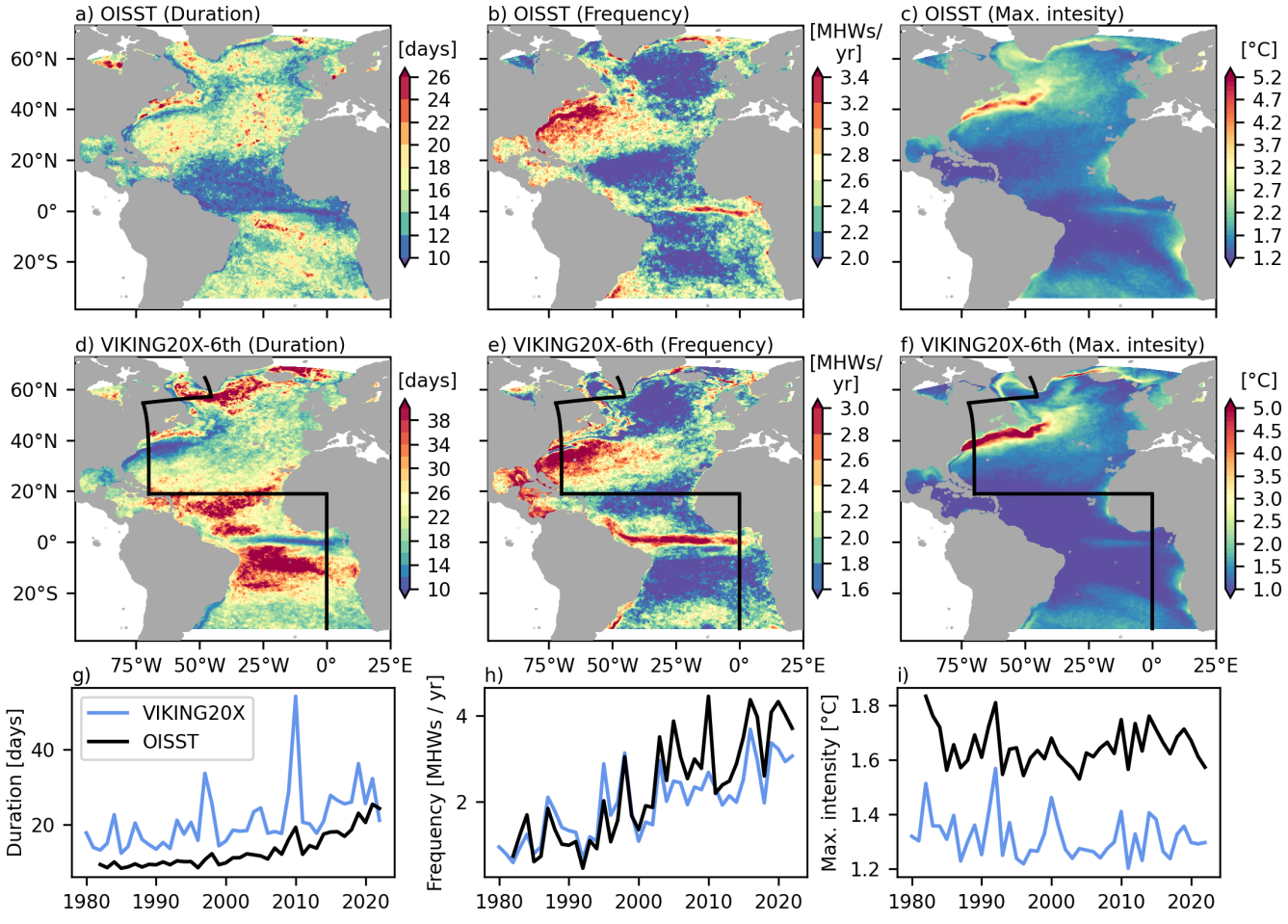

Figure 4. Mean (1982-2022) duration, frequency and maximum intensity of MHWs at the surface in the NOAA OISST dataset (a-c) and the 6th cycle of VIKING20X (d-f). The black line in d-f indicates the section shown in figure 5. Timeseries show the annual mean MHW characteristics averaged over the Atlantic from both datasets (g-i).

3.2.2 Characteristics of MHWs at depth

A broken section through the Atlantic (see black lines in figure 4d-f) shows that the characteristics of MHWs considerably vary in the horizontal, as well as in the vertical plane (figure 5). MHWs in the abyssal ocean last long, but occur rarely. This is directly related, as MHWs that last a year can, by definition, only occur once a year. The only exception is the eastern subtropical gyre, between Puerto Rico and Canada, where relatively short MHWs occur at abyssal depth. However, the abyssal ocean may not have fully adjusted even after more than 300 model years. Therefore, the abyssal ocean should be interpreted

https://doi.org/10.5194/egusphere-2025-571
Preprint. Discussion started: 17 February 2025

with caution. Another maximum in MHW duration occurs between 1000 and 2000 m. In the subpolar gyre the depth range extends from 300 to 3000 m depth.

There is a general tendency for longer MHWs to coincide with a lower frequency, but compared to the duration, the frequency shows stronger differences along the section at the same depth level. The frequency is higher along the boundaries in the eastern upwelling regions (around Africa) and within the western boundary currents. Here the highest frequency is not reached at the surface, but between 500 and 1000 m depth. In the subpolar gyre the maximum frequency is reached even deeper.

The maximum intensity peaks at the surface along the entire section. Outside the tropics, a secondary maximum occurs at depths around 500 m. Below 1000 m, the maximum intensity does not exceed 0.1°C in most regions. Within energetic currents, for example the Deep Western Boundary Current (DWBC) close to Puerto Rico and the GS, the intensity is higher and can reach up to 0.2°C even beyond 3000 m depth (figure 5c). Also around the Mid-Atlantic Ridge, the maximum intensity is elevated. In the deep convection region in the western subpolar gyre the maximum intensity is higher than 0.1°C down to 2500 m depth.

Overall, the sections show that MHWs are more frequent and intense in regions of strong current variability and/or strong gradients in mean temperature. The presence of deep currents leads to pronounced sub-surface maxima in frequency and intensity, with a tendency for comparably short MHWs. Variability linked to deep convection in the central Labrador Sea causes intense MHWs below 1000 m depth as well, but they last longer and occur less frequent than MHWs along the deep boundaries.

Many studies and the VIKING20X model agree on an increase in MHW frequency, duration and intensity at the surface (Xu et al., 2022; Oliver et al., 2018; Chiswell, 2022). The magnitude and sign of linear trends is not uniform across the ocean, however. The duration of MHWs increased in the tropical and central subtropical gyre between 500 and 1500 m depth (crosses in figure 5). The South Atlantic shows a significant decrease (dots in figure 5) in duration below 2000 m, while the subtropical North Atlantic only shows such a decrease between 2000 and 3500 m. Regions of positive trends in duration are also subject to a positive trend in frequency and maximum intensity. This may seem to contradict the previous description, as MHWs in regions of higher mean frequency tend to be shorter. At the same time it is expected, since a warming leads to the threshold being exceeded more often and for longer. A distinct pattern can be seen in the subpolar gyre. Here positive trends in all characteristics occur at the surface and negative trends around 3000 m, which can be explained by a reduction in deep convection. A near-surface warming increases the MHW intensity, duration and frequency, but also the mixed layer depth. The shallower winter mixed layers then prevent mixing between the deep waters (that are no longer reached by the mixed layer) and the upper ocean waters. Below 3000 m the boundary currents are colder than the interior Labrador Sea, likely causing a cooling in the absence of exchange with the surface.

https://doi.org/10.5194/egusphere-2025-571
Preprint. Discussion started: 17 February 2025

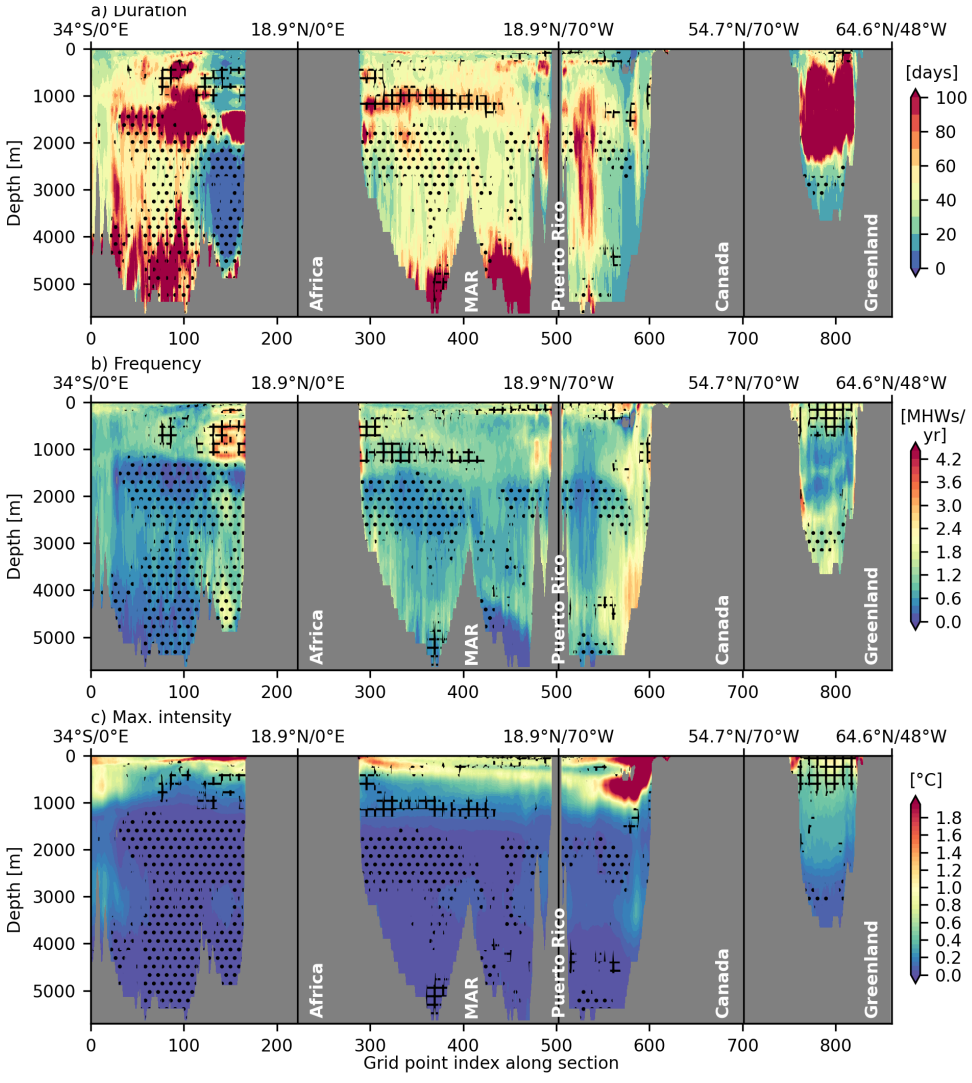

Figure 5. Mean (1980-2022) duration, frequency and maximum intensity of MHWs along a section through the Atlantic Ocean (see figure 4) based on the 6th cycle of VIKING20X and applying the WMO baseline (shading). The sign of the linear trend (1980-2022) at the same grid points is indicated by crosses (positive trend) and dots (negative trend). They are only drawn where the trend is significantly different from zero based on a 5% significance level.

3.2.3 Bottom marine heatwaves

As the seafloor provides a unique habitat for various marine species, the detection of MHWs along the seafloor rather than a fixed depth is of major interest for the biological community. Bottom MHWs are defined here as MHWs that occur in the last ocean filled model grid cell above the bottom.

https://doi.org/10.5194/egusphere-2025-571
Preprint. Discussion started: 17 February 2025

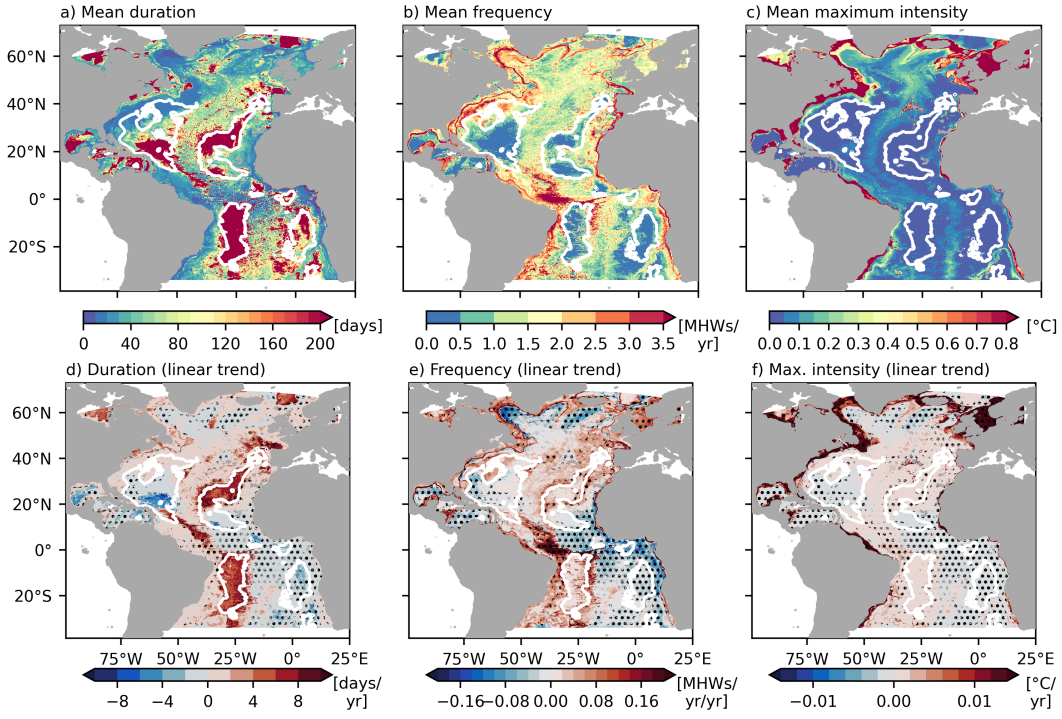

Figure 6. Mean (1980-2022) duration, frequency and maximum intensity of MHWs at the bottom (WMO baseline; VIKING20X-6th nest grid; a-c). The linear trend is shown in the lower panels (d-f). Significant trends (5% significance level) are indicated by dots. A bottom depth of 5000 m is indicated by the white contour.

The deep ocean basins with depths exceeding 5000 m are characterised by very long, but infrequent MHWs (figure 6a-c). The duration of MHWs exceeds a year and therefore the low frequency is a direct consequence, as already mentioned above. Also, the bottom water masses are potentially still subject to model drift even after more than 300 years of model spin-up, which leads to a near permanent heatwave state in the beginning or end of the timeseries. Although, their maximum intensity remains below 0.1°C, the temperature tolerance of most deep sea species is highly uncertain and the possible impact of such low intensity, but long lasting MHWs, yet to be determined. It is interesting to note that, even though very deep, the North American Basin is characterised by rather short MHWs. This suggests that the high variability associated with the GS impacts temperature extremes down to the sea-floor. In general, MHWs are shorter near and along the continental slopes compared to the interior ocean and Mid-Atlantic Ridge, even if the sea-floor is located at similar depths. The frequency of bottom MHWs is highest along the continental slope. Notably it is higher along the slope than it is on the shelf, which is related to the subsurface maxima along the slope seen in figure 5. High frequencies are seen along the western boundary following the DWBC pathway, along the pathways of the overflow water in the subpolar gyre and along the eastern boundary. The maximum intensity strongly follows the bathymetry with highest intensities reached on the shelf. Further, the intensity is higher along seamount chains and the Mid-Atlantic Ridge where the sea-floor is elevated.

https://doi.org/10.5194/egusphere-2025-571
Preprint. Discussion started: 17 February 2025

Bottom MHWs on the shelves show an increase in frequency, duration and maximum intensity over time (figure 6d-f). The linear trend is not significant everywhere on the shelf and along the upper continental slope, due to strong interannual variability. Significant positive trends in deeper ocean regions can be seen in the eastern subtropical North Atlantic and the western tropical Atlantic. Significant negative trends can be seen in the subpolar gyre, Caribbean Sea and in the entire eastern tropical and subtropical South Atlantic. Again, trends in the deep ocean are associated with higher uncertainties, due to the lack of long-term observations and in particular the abyssal plains may be still subject to model drift.

3.3 The impact of mesoscale dynamics on the characteristics of MHWs

The previous sections suggest that the presence of strong and highly variable currents has an important impact on the characteristics of MHWs. To test how the representation of mesoscale dynamics impacts the characteristics of MHWs, we compare the 6th cycle in VIKING20X to the 6th cycle in the un-nested ORCA025 configuration. The higher horizontal resolution leads to the presence of individual mesoscale features in VIKING20X, of which only a small part is simulated in ORCA025 outside the subtropics (Biastoch et al., 2021). It also leads to changes in the mean current structure and position, as well as differences in temperature trends and in horizontal and vertical temperature gradients (figure A1). All these aspects may have an impact on the characteristics of MHWs.

The VIKING20X dataset contains the imprint of mesoscale dynamics throughout the Atlantic as discussed above, although for both configurations MHWs are detected on a 1/4° grid. Results are only shown for the WMO baseline, but the conclusions do not depend on the baseline.

At 1000 m depth VIKING20X shows a high frequency of MHWs along the western and eastern boundaries as well as along the equator (figure 7a). Compared to ORCA025 the frequency in VIKING20X is higher almost everywhere, but in particular along the western boundary and eastern boundary outside the tropics (figure 7c,e). At the western boundary this goes along with a stronger, more narrow and more variable western boundary current in VIKING20X. This is apparent by the difference in mean and eddy kinetic energy (MKE/EKE) in the two configurations (figure A1). Also vertical velocity fluctuations (vertical velocity EKE) are stronger along the western boundary in VIKING20X. Along the eastern boundary differences in MKE are relatively small, but EKE is still higher at least north of the equator. Also the horizontal and vertical temperature gradients are larger in VIKING20X (figure A1). When averaged over the entire Atlantic, the temporal evolution of the MHW frequency is similar, but the mean frequency is clearly higher in VIKING20X. Although it is not possible to prove that the higher frequency in VIKING20X is more realistic, it is expected that the more realistic representation of currents and their variability leads to more realistic MHW characteristics in VIKING20X.

The maximum intensity shows a strong maximum in the region of the GS separation at 34°N (figure 7b). Also in the eastern Atlantic between 40°N and 60°N the mean maximum intensity exceeds 1.2°C. In this area, the transition between the warm Mediterranean Sea Outflow Water and colder North Atlantic Deep Water is located at approximately 1000 m depth (Kaboth-Bahr et al., 2021; Liu and Tanhua, 2021), suggesting that a large vertical temperature gradient could be the cause for the high MHW intensity. High values of maximum intensity are further seen west of Greenland, where the flow instabilities lead to

https://doi.org/10.5194/egusphere-2025-571
Preprint. Discussion started: 17 February 2025

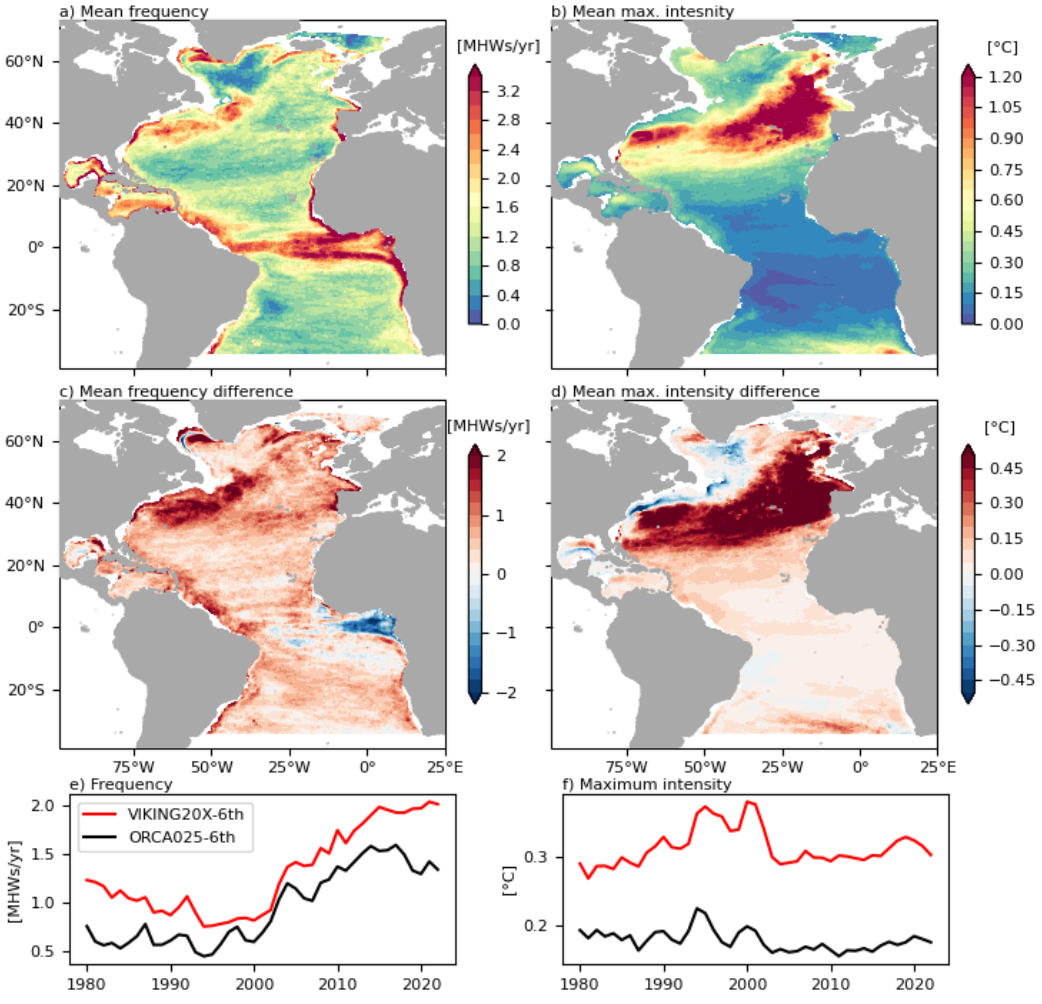

Figure 7. Mean (1980-2022) MHW frequency and maximum intensity at 1000 m depth in the 6th VIKING20X cycle (a,b). Difference between VIKING20X (6th cycle) and ORCA025 (6th cycle) (c,d). Timeseries show the average over the Atlantic from both experiments (e,f). In all panels MHWs are defined using the WMO baseline.

the shedding of West Greenland Current eddies and Irminger Rings, which are typical expressions of the mesoscale resolution in this region (Biastoch et al., 2021; Rieck et al., 2019). Along the western boundary, south of the DWBC/GS crossover, the maximum intensity is higher than in the interior as well. Compared to ORCA025, VIKING20X simulates more intense MHWs (figure 7d,f). The difference is strongest in the regions where the mean maximum intensity is highest. West of Greenland this is directly linked to the presence of mesoscale eddies in VIKING20X as discussed above. The presence of Irminger Rings that transport warm water from the Irminger Current into the cold central Labrador Sea in VIKING20X is likely related to the occurrence of strong MHWs. The negative difference north and positive difference south of the GS pathway suggests a more southern position of the GS in VIKING20X. This is supported by the MKE and horizontal temperature gradient differences

https://doi.org/10.5194/egusphere-2025-571
Preprint. Discussion started: 17 February 2025

(figure A1). Higher intensities are seen along most of the western boundary related to a stronger horizontal temperature gradient and higher EKE. In the eastern North Atlantic the vertical temperature gradient is stronger in VIKING20X, which can explain the higher maximum intensities. As explained above, the vertical temperature gradient is strongly influenced by the properties of the Mediterranean Sea outflow in this region. The reason for the different stratification may not be directly related to the representation of the mesoscale, but it demonstrates the importance of the outflow properties on the characteristics of MHWs in the eastern mid-latitude North Atlantic.

Overall, the more realistic representation of boundary currents, coastal upwelling and the ability to resolve sharper temperature gradients leads to a higher frequency (and shorter duration) and higher maximum intensity of MHWs throughout most of the Atlantic, but in particular along the western boundary. This was only shown for the depth of 1000 m, but similar arguments apply at least to the depth range from 300 to 3000 m. This means that studying the impact of MHWs on deep ecosystems along the continental slopes requires models with sufficiently high resolution. Away from the boundaries the model resolution is particularly important along the GS and North Atlantic Current (NAC) pathway throughout the entire water column.

3.4 Vertical structure and drivers of marine heatwaves in an example region

In order to better understand the vertical structure and coherence of MHW events, we now focus on the Cape Verde archipelago in more detail. The Cape Verde archipelago is located in the eastern tropical Atlantic in between the westward flowing North Equatorial Current and eastward North Equatorial Counter Current. It is part of the Canary Current upwelling system and thus characterised by large-scale upwelling (Arístegui et al., 2009; Cropper et al., 2014).

This region is selected here as an example, due to its high species richness, including the presence of vulnerable marine ecosystem (VME) indicator species (Vinha et al., 2024; Hoving et al., 2020; Stenvers et al., 2021) and large bottom depth gradients (see figure 8) such that benthic ecosystems span a large depth range in a horizontally confined region. As a result, one might expect MHWs to have important impacts beyond the surface and thus a detailed understanding of their characteristics throughout the water column is highly relevant. Furthermore, the eastern subtropical Atlantic was identified as a region of significant positive trends in the MHW characteristics in approximately the top 1000 m and negative trends below (figure 5).

The characteristics of MHWs at the surface do not vary in phase with the characteristics of MHWs below approximately 50 m depth (figure 9). Already at 100 m depth the explained variance has dropped to values below 25%. This means that the surface heat flux accounts for only a small fraction of the variance in the MHW characteristics. This is consistent with impact of surface forced trends being limited to about 50 m depth in the Cape Verde archipelago as discussed above (figure 3). Removing the linear trend of the MHW characteristics itself, or detecting MHWs with a linear baseline leads to the same results. It is therefore not just different long-term trends that decouple surface MHWs from deeper MHWs, but also different characteristics of variability on shorter timescales.

https://doi.org/10.5194/egusphere-2025-571
Preprint. Discussion started: 17 February 2025

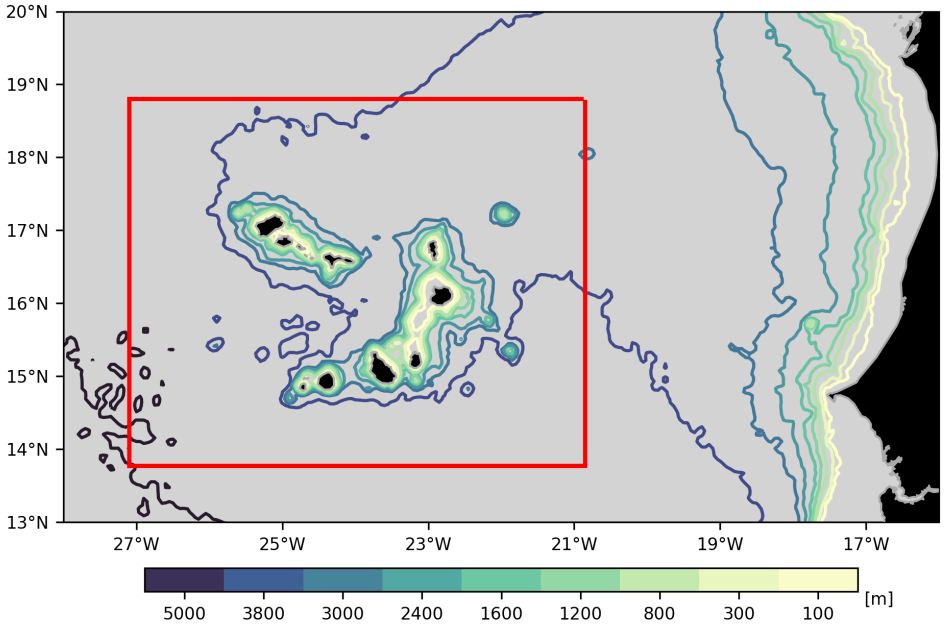

Figure 8. Depth of the seafloor in the eastern tropical Atlantic. The Cape Verde archipelago region (red) is used for the spatial averages in figures 9, 10 and 11.

Annual mean duration, frequency and maximum intensity are subject to pronounced interannual variability near-surface. In deeper layers low frequency variability is more dominant (figure 9), which leads to a lower explained variance. In the late 2000s an increase in MHW duration, frequency and maximum intensity seems to propagate from the surface towards sub-surface layers above 300 m. Thus, there might be a connection between surface MHWs and MHWs in the upper 300 m even though they don't have the same characteristics, nor appear at the same time. The maximum intensity is scaled with the difference between the climatological mean and 90th percentile here to compare the anomaly to the magnitude of local variability, which is much lower in the deep ocean. It is interesting to note that the absolute maximum intensity is much stronger near-surface (see for example figure 5), but the scaled intensity shows similar values at all depth levels (figure 9). This means relative to the typical range of variability, MHWs are similarly intense at all depths.

Between 300 and 1200 m MHW characteristics are mostly in-phase between with low values in all variables before 2000 and higher values afterwards. For this depth range no connection to the surface can be identified, even when possible time delays are considered. Between 1200 m and 3000 m strong and intense MHWs occur frequently at the beginning of the timeseries and nearly no MHWs occur after 1995. Between 3000 and 4000 m MHWs do not show a considerable trend, but more variability on interannual timescales. It is important to note that the MHW definition was applied at individual grid points and depth levels and does not include any spatial information. Still, the characteristics of MHWs vary in phase over larger depth ranges, even though mostly not connected to the surface, but other processes that act coherently over a certain depth ranges. These processes

https://doi.org/10.5194/egusphere-2025-571
Preprint. Discussion started: 17 February 2025

are investigated in more detail in the following.

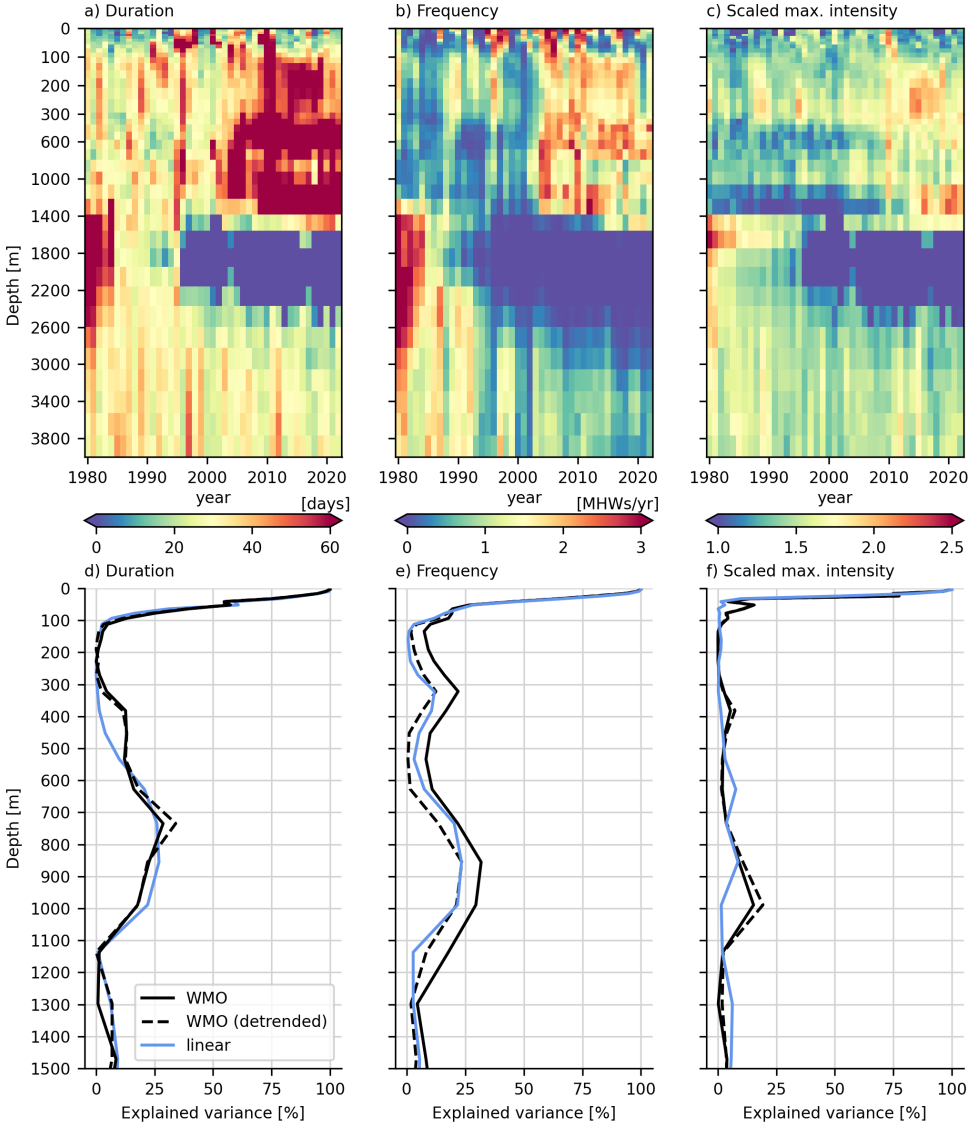

Figure 9. Annual mean MHW duration, frequency and scaled maximum intensity in the Cape Verde archipelago (WMO baseline; VIKING20X-6th; a-c). Explained variance of the MHW duration, frequency and scaled maximum intensity at different depth by their annual mean values at the surface (d-f). The explained variance was calculated for the WMO baseline (black, solid), the WMO baseline but with the trend removed after calculating the annual mean MHW characteristics (black, dashed) and for the linear baseline (blue).

In order to understand which drivers control the variations of MHW characteristics at different depth, we consider individual MHW events and investigate the daily fraction of the total area that is covered by a MHW relative to the entire area of the Cape

https://doi.org/10.5194/egusphere-2025-571
Preprint. Discussion started: 17 February 2025

Verde archipelago (figure 10). The mixed layer is characterised by intermittent events where most of the area is in a MHW state. High MHW coverage often only persists for a few months. After 1995 high MHW coverages above 70% persists for longer, sometimes more than a year. By comparing the results from MHWs detected using the WMO and linear baselines, it is evident that the linear trend in the mixed layer had a minor impact in the Cape Verde archipelago. The timing and coverage of MHWs is similar (figure 10a,b). The mixed layer (here maximum mixed layer within the region) shows a seasonal cycle from 20 m in summer to 100 m in winter. In several years (e.g. 1995, 1998, 2002, 2010) MHWs occur in the mixed layer when it is deep during winter and remain below the mixed layer as it shoals in summer. While MHWs are then often terminated in the mixed layer, presumably due to surface fluxes, they persist below. This leads to different characteristics of MHWs in the top 50 m and the depth layer between 50 and 100 m, but MHWs may still be initially forced by a heat gain through the surface.

Below 100 m only in few years (e.g. 1992, 2010) a high MHW coverage at the surface seems to propagate to 300 m depth in the following years. However, the depth range between 100 and 300 m is clearly not only governed by the surface exchange of heat, but other processes as well. The MHW coverage shows a stronger positive trend in this depth range compared to the surface. MHWs detected based on the linear baseline also show an increase after 2004, but the coverage is generally lower. This indicates that both, decadal variability and a long-term trend, cause the strong increase in MHW coverage seen with the WMO baseline. In several years the MHW coverage exceeds 50% without any MHWs occuring at the surface during the same or previous years, independent of the baseline used.

Between 300 and 1200 m only few MHWs occur before 2005, but the MHWs coverage continuously exceeds 70% afterwards. This layer is split by a thin layer of nearly zero MHW coverage even after 2005. When applying the linear baseline, the depth ranges between 300 and 800 and 800 to 1200 m seem to be more disconnected. This suggests that the apparent coherence when applying the WMO baseline is mostly caused by a similar temperature trend, while variability on shorter timescales has different timings.

From 1200 m to 2200 m depth a high MHW coverage is seen until 1985 and nearly no MHWs afterwards (WMO baseline). Using the linear baseline, MHWs additionally occur after 2010. This depth range is characterised by a long term cooling trend, as well as multi-decadal variability that reached a high phase in the 1980s and 2010s. Below 2200 m intermittent high MHW coverage occurs throughout the entire timeseries. Long-term trends are of minor importance in this depth range, apparent by the similarity between the WMO and linear baselines.

In general, the main results derived from the annual mean MHW characteristics are directly represented in the daily MHW coverage. MHWs can extend beyond the mixed layer, but they are not in-phase with surface MHWs and persist longer. Beyond 300 m depth, coherent MHWs occur over layers a few 100 to 1000 m thickness (figure 10c,d). While coherent within the layer, the occurrence of MHWs does not seem to be related across layers, due to different long-term trends and different timing of interannual to decadal variability. Depth levels that show coherent variability are mostly independent of the baseline used. The only notable difference is that the explained variance profile of the MHW coverage in 450 m depth shows a secondary maximum at 1100 m depth when the WMO baseline is applied. This secondary peak is missing for the linear baseline. As explained above this is caused by similar trends, but different timing of interannual to decadal variability. It is important to note that the

https://doi.org/10.5194/egusphere-2025-571
Preprint. Discussion started: 17 February 2025

described temporal changes in MHW characteristics apply to the entire archipelago region and are not related to processes that only occur close to the islands for example.

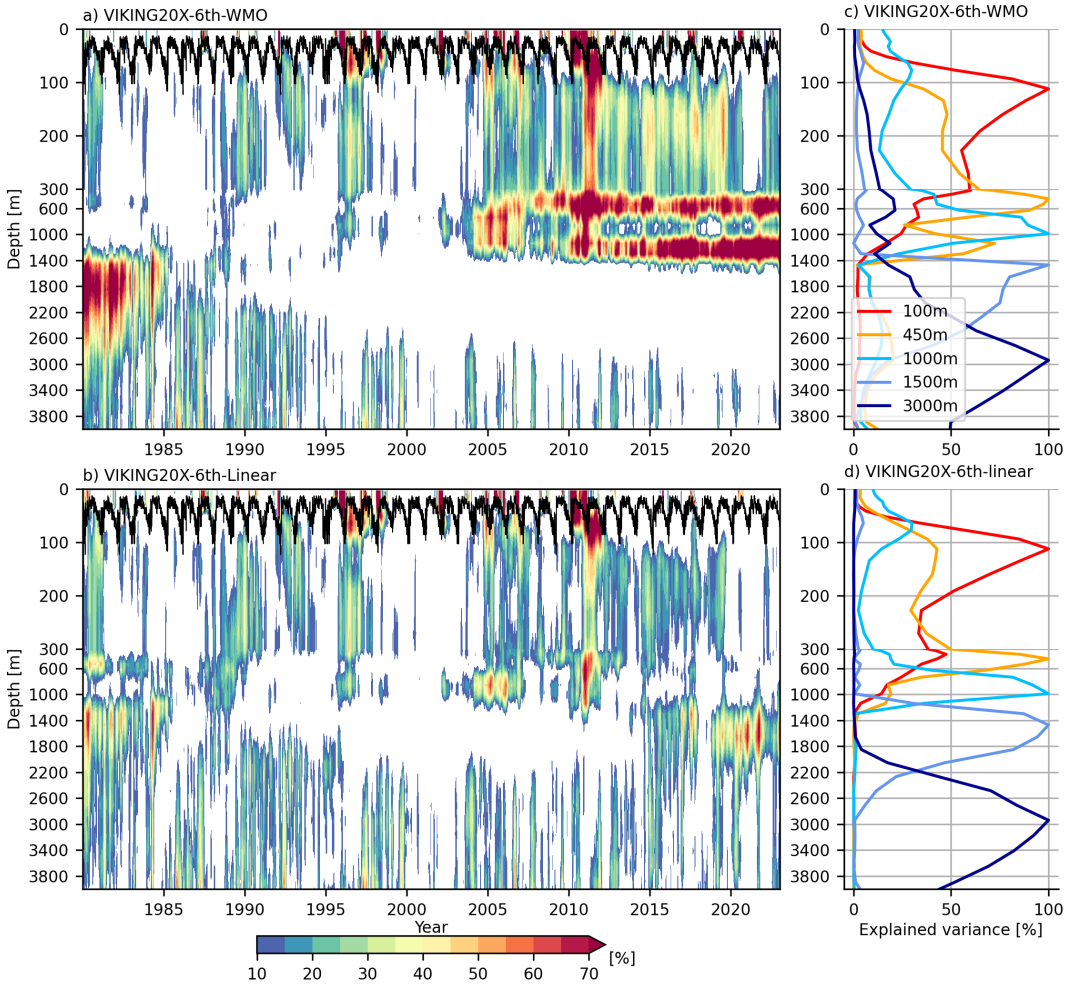

Figure 10. Fraction of the area in the Cape Verde archipelago that is occupied by a MHW on any given day in the 6th cycle of VIKING20X when applying the WMO (a) and linear (b) baselines. Values smaller than 10% are not shaded. The black line indicates the maximum mixed layer depth within the region. Vertical profiles of the MHW coverage variance explained by its values in 5 selected depths (c,d).

As none of the depth levels below 300 m show any hint on connections to the surface, oceanic processes are responsible for the development and characteristics of these deeper MHWs. To understand what causes MHWs and what sets the vertical extend of coherent MHWs we calculate a heat budget for the Cape Verde archipelago. As expected, the MHW coverage closely follows the heat content integrated over the region (figure 11a). The heat content shows pronounced interannual variability at the surface, a long-term positive trend between 100 and 1400 m depth and a negative trend below 1400 m that becomes small

https://doi.org/10.5194/egusphere-2025-571
Preprint. Discussion started: 17 February 2025

below 3000 m depth. This structure is also reflected in the mean heat content change between 1980 and 2022, which itself is caused by a residual of much larger heat fluxes (figure 11c). At the surface the ocean gains heat trough the air-sea heat fluxes. This heat is transferred to deeper levels by mixing, which is part of the residual flux. At the base of the mixed layer the vertical heat advection term shows a positive maximum, indicating that the ocean gains heat through vertical heat convergence in this depth range. The horizontal convergence of the heat transport counteracts the vertical transport at all depth levels and cools the ocean between 50 and 200 m. Between 200 and 600 m the opposite is true. Here upwelling of colder water from depth leads to a mean cooling, balanced by a horizontal convergence of heat. Below 600 m the mean fluxes become very small compared to their near-surface values. While the terms are balanced in the mixed layer, there is small residual that leads to a heat content change (and causes a linear trend in the OHC, when integrated over time). Even though the sign of the vertical and horizontal heat convergence alternate with depth, the residual grows until 1200 m and becomes negative at 1500 m. This suggests that it is not a single mechanism that leads to the trend.

When removing the impact of the linear trend, MHWs typically occur following periods of sustained positive heat content change (figure 11b). However, this must not always be true since a strong heat content increase will not result in a MHW, if the ocean is anomalously cold before. As for the MHW coverage, the heat content change does not vary in phase across the entire water column. The layers in which MHWs occur at the same time are strongly related to the processes that cause the heat content to vary at different depths (figure 11d, 10c,d). Within the mixed layer (above 50 m) heat content variability is dominated by vertical mixing of heat that is gained trough the surface. At the base of the mixed layer most of the heat content variance is explained by vertical heat advection. Between 300 and 700 m lateral and vertical heat advection explain similar fractions of the variance, while between 800 and 1300 m the vertical term reaches 70% explained variance. Between 1600 and 2400 m it is the horizontal heat convergence that dominates heat content variability. Below 2400 m it is again the vertical advection that becomes more important.

The different relative importance of the vertical and lateral heat convergence are in turn related to the vertical structure of the currents and temperature field. In the mixed layer horizontal currents are strong, but the temperature gradient across the domain boundary is small. At the base of the mixed layer, the speed of horizontal currents is already only a small fraction of their surface value (although still much larger than vertical velocities in absolute terms). Here the vertical temperature gradient reaches a maximum, explaining the high importance of vertical advection. Between 300 and 700 m the horizontal temperature gradient reaches a maximum, but also the vertical speed is comparably large. Therefore both, horizontal and vertical heat transports, contribute to heat content variations. Below 700 m the horizontal temperature gradient is small again, while vertical velocities and vertical gradients still reach more than 10% of their maximum value and therefore have a larger impact. Note that around 800 m depth, which appears as a level with distinct variability as explained above, the mean horizontal temperature gradient becomes negative. Thus a vertically coherent circulation change will lead to opposite signed heat content changes in different depths. Between 1600 m and 2300 m the vertical temperature gradient reaches near-zero. This is where the contribution of vertical advection becomes negligible. Below 2700 m depth the vertical temperature gradient grows slightly. In the presence of comparably large vertical velocities this causes the vertical heat transport to be again important for the generation of heat

https://doi.org/10.5194/egusphere-2025-571
Preprint. Discussion started: 17 February 2025

content changes. Therefore, the changing relative importance of the vertical heat transport (figure 11d) is mostly caused by changes in the vertical temperature gradient. In 1000 and 3000 m depth, where the vertical heatflux has a major contribution to heat content changes, enhanced vertical gradients can be seen across the entire domain (not shown). Thus, the large-scale temperature stratification rather than local effects close to the islands set the vertical structure of coherent MHWs.

In conclusion, MHWs in the Cape Verde archipelago are related to surface fluxes in the top 100 m of the ocean. This includes the mixed layer, but MHWs can extend beyond the mixed layer through subduction. Even though MHWs are detected at individual grid points and depth levels, coherent structures can be identified. The depth range over which coherent MHWs occur are closely related to the vertical and horizontal structure of the temperature field. Both, horizontal and vertical heat advection play a major role. Changes in their relative importance, which are primarily linked to vertical changes in the large-scale temperature stratification, set the depth ranges over which coherent MHWs occur. If the linear baseline is applied, the detected MHWs are related to pentadal to decadal variability at depth, while applying a fixed (WMO) baseline results in a combination of both, pentadal to decadal variability and the long-term temperature trend. Nevertheless, the different baselines yield similar depth ranges, over which MHWs occur at the same time. The described processes act over the entire archipelago and are not related to processes that occur along the island slopes for example.

https://doi.org/10.5194/egusphere-2025-571
Preprint. Discussion started: 17 February 2025

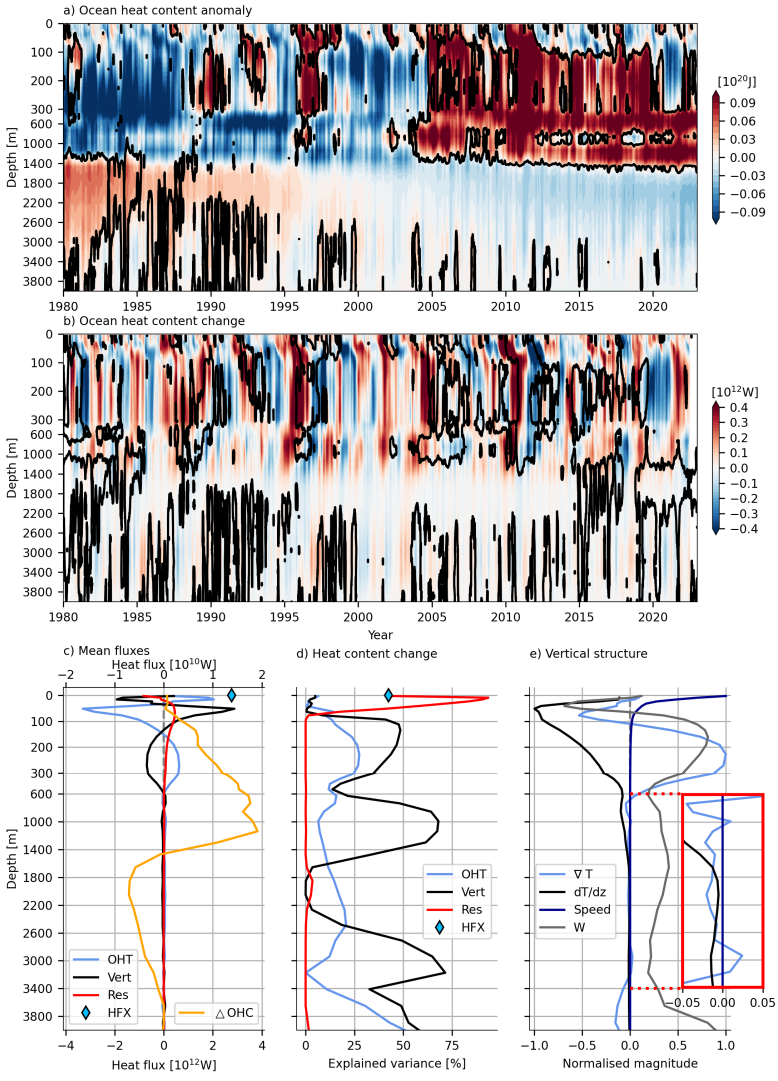

Figure 11. Ocean heat content anomaly in the Cape Verde archipelago and 15% MHW coverage contour based on the WMO baseline (VIKING20X-6th; a). Day to day ocean heat content change and 15% MHW coverage contour based on the linear baseline (VIKING20X-6th; b). Vertical profiles of the mean (1980-2022) heat fluxes from horizontal/vertical ocean advection (OHT/Vert), the surface heat flux (HFX) and the residual (Res) that is mostly related to vertical mixing. The resulting mean ocean heat content change (△OHC) is shown in orange and its values are indicated on the top x-axis (c). Fraction of the heat content change variance explained by different heat budget terms for all depth levels in the model (d). A 10-day running mean was applied to remove high frequency variability. Normalised magnitude of the horizontal temperature gradient (∇T) and speed across the boundaries of the Cape Verde archipelago and average vertical temperature gradient (dT/dz) and vertical velocity (W) within the region. The inlet shows the same, but with different x-axis limits.

https://doi.org/10.5194/egusphere-2025-571
Preprint. Discussion started: 17 February 2025

4 Discussion and Conclusion

4.1 Detecting MHWs at depth

In this study we have analysed the characteristics of temperature extremes (MHWs) throughout the entire Atlantic Ocean. By using a hierarchy of ocean model grids we identified the impact of the horizontal resolution, ocean dynamics and different baselines on the derived MHW statistics.

We find that interpolation of the temperature from a 1/20° to a 1/4° grid does not impact the derived statistics. This is important for the interpretation of model results, but has further implications for the detection of MHWs from gridded observational products. The reason for this result is likely that MHWs do not occur at isolated grid points, but almost always cover an area that is larger than the grid resolution of the datasets (mostly 1/20° to 1/4°). Thus, as long as the target grid size is still small enough to capture the typical extend of MHWs in the region, it is expected that the horizontal resolution of the temperature dataset does not affect the MHW statistics. This would also mean that the interpolation of high-resolution along track data onto a regular, coarser grid does not impact the detection of MHWs.

However, statistics change if the horizontal resolution of the grid affects the dynamic scales resolved in a model. The coarser resolution model with otherwise same surface forcing and initial conditions generally overestimates the duration and underestimates the frequency and intensity of MHWs. This result is consistent with a coupled model study conducted by Pilo et al. (2019). Coarse horizontal resolution is often mentioned as a limiting factor in MHW studies (e.g. Hövel et al., 2022). In the presence of highly variable currents and at mid-depths (100 - 3000 m) differences between the high and coarse resolution configurations can be substantial. Differences are overall small at the surface, except for the NAC region, but the discrepancy is expected to be larger for coarser 1/2° and 1° models (Pilo et al., 2019).

While Hobday et al. (2016) mention that horizontal and temporal resolution of the temperature dataset are important, we argue that the horizontal resolution (in certain limits that are probably related to the typical extend of MHWs) plays a minor role, as long as the dynamics represented in the dataset are the same. As a result, the two-way nesting applied here provides a convenient tool to produce a manageable dataset containing mesoscale effects. Note that detecting MHWs on the high resolution grid requires approximately 25 times more computing time and significantly more resources for analysis and storage. Daily MHW statistics for 43 years on all 46 depth levels on the coarse grid (only the domain covered by the nest) take up 90 GB of storage, while it is 700 GB on the high-resolution grid. The amount of data that needs to be processed is even higher, since the output file size is strongly reduced by compression.

The choice of a suitable baseline is widely discussed in the current literature and depends on the scientific question (Amaya et al., 2023b). Modelled temperature trends can strongly differ across experiments, for example dependent on the time of the model spin-up (adjustment to initial conditions). While trends are robust in approximately the top 100 m, they strongly depend on the time of the model spin-up at greater depths. Trends at depth vary in magnitude and even have opposite signs in our model experiments that just differ in the initial conditions. As a consequence, the WMO and fixed baselines are not applicable

https://doi.org/10.5194/egusphere-2025-571
Preprint. Discussion started: 17 February 2025

below approximately 100 m in the presence of strong model drift. This is not only a question of interpretation, but the slow adjustment of the deep circulation does not allow for any meaningful interpretation of the results. We have investigated this in only one model configuration here, but model drift is common to nearly all forced and coupled models (e.g. Tsujino et al., 2020). As a consequence, if the aim is to include multi-decadal trends in the MHWs statistics at depth, a model spin-up with sufficient time to allow the deep-ocean to equilibrate is needed (around 200 years in VIKING20X). For the abyssal basins with water depths beyond 5000 m the comparison of the WMO and linear baselines suggest that an even longer spin-up is necessary. Such a long spin-up is often not feasible at this resolution. Nevertheless, it was shown that at the surface, where both cycles are dominated by the surface forcing, similar results are obtained. Studies that focus on near-surface MHWs get away with using a much shorter spin-up, as the ocean model typically stabilises quickly. Additional constraints to reduce model drift, such as the assimilation of observations, could also alleviate the problem, while at the same time acknowledging the fact that deep observations are sparse. Ocean reanalysis was successfully used by Fragkopoulou et al. (2023) to study MHWs at depth. Nevertheless, frequent and widespread observations typically exist only in the top 1000 m and thus also reanalysis products should be treated with caution in the deep ocean. Furthermore, a downside of many assimilation techniques, in particular of nudging, is that they may violate conservation laws (Zeng and Janjić, 2016; Janjić et al., 2014) and thus studying the drivers of MHWs is problematic in such datasets due to spurious sources and sinks of heat.

4.2 Characteristics, drivers and trends

From their definition it immediately follows that MHWs need to occur everywhere (disregarding the condition that the temperature threshold must be exceeded for 5 consecutive days). Therefore, the pure observation that MHWs occur throughout the entire water column is not surprising. Still, the detection of MHWs is a useful tool to comprehensively study the characteristics of temperature variability and how it changes in time. In the upper ocean temperatures cover a large range and anomalously high temperatures occur for relatively short times. In the deep ocean temperature anomalies associated with MHWs are smaller and occur on longer timescales compared to the surface. Along the continental slope MHWs with maximum intensities in the order of 1°C do occur. Given that the temperature tolerance of deep-sea species like cold-water corals is expected to be around 4°C (Morato et al., 2020), this could have major impacts for ecosystems that are already close to their upper temperature limit. In the abyssal ocean MHWs intensities do not exceed 0.1°C. Whether such low temperature variations have any impact is yet to be investigated. In general, even small temperature anomalies could have an impact, if they are sustained for sufficiently long times. At the same time, ecosystems may have adapted to large temperature variability in regions where MHWs occur very frequently and thus do not represent rare events. The aim of this study is to provide a comprehensive understanding about the characteristics of temperature variability throughout the entire Atlantic which, when combined with biological information, will help to identify deep ecosystems that may be vulnerable to MHWs and changes in their characteristics.

Overall, our results highlight the importance of the ocean circulation on the development and characteristics of MHWs. By comparing two model configurations that only differ by their horizontal resolution, we find that mesoscale dynamics change the frequency, duration and maximum intensity of MHWs, in particular at depth. In agreement with Großelindemann et al.

https://doi.org/10.5194/egusphere-2025-571
Preprint. Discussion started: 17 February 2025

(2022); Zhang et al. (2023); Elzahaby and Schaeffer (2019); Wyatt et al. (2023) and Wu and He (2024) this is partly caused by mesoscale features such as eddies and meanders themselves. Additionally, indirect effects, such as changes in current structure, strength, mixed layer dynamics, and vertical as well as horizontal temperature gradients contribute to differences between the eddy-permitting and eddy-rich configurations in our study. Highly variable currents, such as the NAC and DWBC are related to the occurrence of short, but frequent MHWs in agreement with Fragkopoulou et al. (2023). Also the Mediterranean Sea Outflow, deep convection in the Labrador Sea and upwelling were found to strongly influence the occurrence and characteristics of MHWs at depth. As the surface forcing can be ruled out as the cause, this points to a major influence of ocean dynamics on the occurrence of MHWs at depth, but also at the surface. In most regions of the Atlantic, the impact of the local surface forcing on MHWs is limited to approximately the top 100 m, with some minor regional differences. Consistent with other studies (Xu et al., 2022; Oliver et al., 2018; Chiswell, 2022) we find a positive trend in all MHW characteristics when applying a fixed baseline at the surface. Although not related to the surface forcing, but changes in ocean dynamics, positive trends can be seen in most regions until a depth of roughly 1000 m. Between 1000 and 4000 m negative trends prevail in the model. Although model trends are always connected to a large uncertainty, in particular in the deep ocean, this result suggests that many deep ecosystems experienced a decrease in extreme (positive) temperatures over time. At the very least the model shows that even though trends are clearly positive at the surface, it can not be expected that marine heatwaves increased over time throughout the water column.

Based on a more detailed investigation of MHWs in the Cape Verde archipelago we find that for the long-term trend, but also for variability on shorter timescales, the depth of approximately 100 m marks a transition zone. This is caused by very different characteristics within and below the mixed layer, which is consistent with results obtained by Scannell et al. (2020) and Amaya et al. (2023a). In agreement with these studies, surface forced MHWs can be detrained from the seasonally varying mixed layer. If they are subducted below the annual maximum mixed layer, they can persist for several years, otherwise they may re-emerge at the surface.

Below approximately 100 - 300 m depth, the surface forcing does not affect MHWs in most regions. Here vertical and lateral ocean heat transports control the heat budget and therefore the occurrence of MHWs. For the Cape Verde archipelago the vertical structure of the temperature field sets the depth range over which vertically coherent MHWs occur. It is an important result itself that vertically coherent MHWs are detected at all, even though the definition is applied to every grid point individually. Although this was studied explicitly only for the Cape Verde archipelago, the Atlantic wide statistics suggest that similar mechanisms occur throughout most of the basin. As a result, our study strongly supports the conclusions of Sun et al. (2023); Zhang et al. (2023); Elzahaby and Schaeffer (2019); Schaeffer and Roughan (2017) and Wyatt et al. (2023) that measuring temperature at the surface alone yields no information on extreme temperature events below the mixed layer. Conversely, studying MHWs at depth will require detailed knowledge of ocean dynamics. This includes vertical velocities that are very small compared to horizontal velocities, but can be very important due to larger vertical than horizontal temperature gradients.

https://doi.org/10.5194/egusphere-2025-571
Preprint. Discussion started: 17 February 2025

In conclusion, this study presents results of a single model simulation, but the main results are consistent with various other publications as described above. The mean characteristics at the surface and at depth are qualitatively and quantitatively similar to the ocean reanalysis based study of Fragkopoulou et al. (2023). As direct observations for a larger domain at daily resolution are not available below the surface, studies of MHWs at depth will have to rely on models in the foreseeable future. This study provides valuable information about the characteristics of MHWs at depth and how they are related to ocean dynamics, as well as a potential pitfalls when detecting deep MHWs in models. Additionally, it provides a unique dataset to launch investigations on the impact of MHWs on subsurface ecosystems.

https://doi.org/10.5194/egusphere-2025-571
Preprint. Discussion started: 17 February 2025

Appendix A: Appendix A

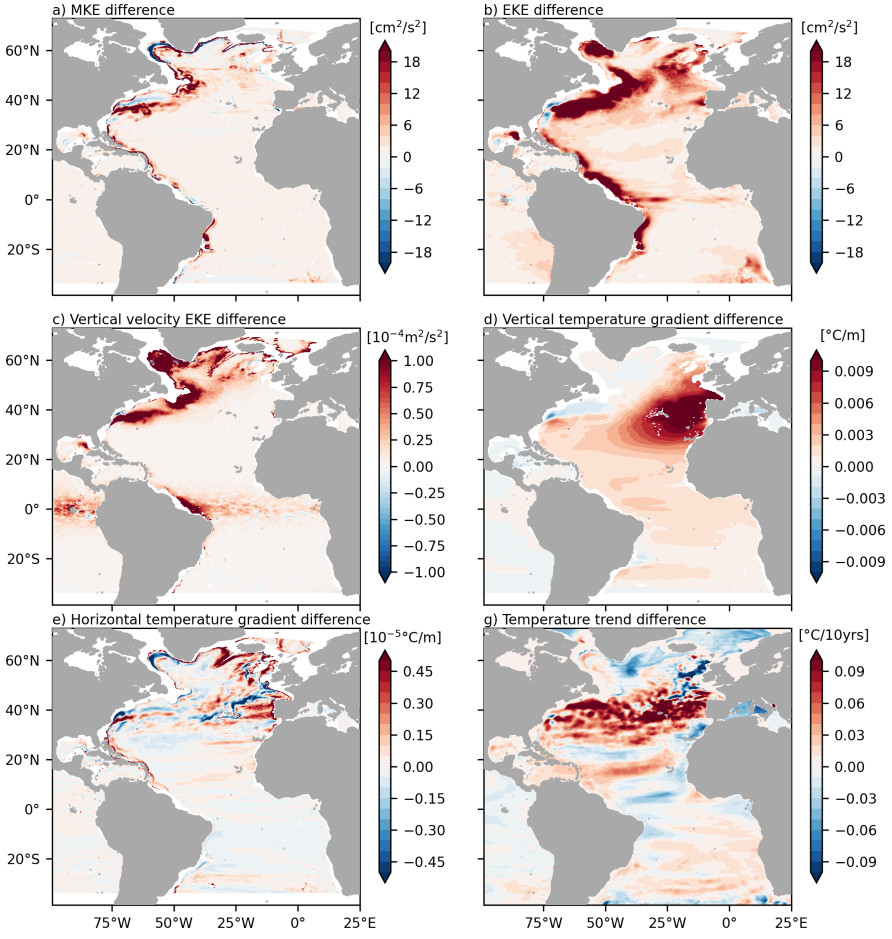

Figure A1. Differences between the coarser resolution ORCA025 and high-resolution VIKING20X configurations. Mean kinetic energy (a), eddy kinetic energy (b), eddy kinetic energy of the vertical velocity (c), vertical temperature gradient (d) and Horizontal temperature gradient (e). All maps show the difference between the mean quantities (1980-2022). The temperature trend (linear regression slope) difference is based on the same time period.

https://doi.org/10.5194/egusphere-2025-571
Preprint. Discussion started: 17 February 2025

Code and data availability. The full MHW detection output for the 6th cycle of VIKING20X is available trough GEOMAR at https://hdl.handle.net/20.500.12085/49913d6b-4c70-43cb-9d3c-b4b73b0b8291 (Schulzki et al., 2025a). Additional data and material that support the findings of this study are available through GEOMAR at https://hdl.handle.net/20.500.12085/a3279a60-e9ef-437f-bd34-c3e156181e98 (Schulzki et al., 2025b)

Author contributions. AB initiated and designed the study. FUS performed the numerical model experiments. All authors contributed to the design of the analysis, which TS performed including the marine heatwave detection. TS wrote the manuscript draft which all authors jointly iterated.

Competing interests. The authors declare that they have no conflict of interest.

Acknowledgements. The study was supported by the European Union's Horizon 2020 research and innovation program under Grant Agreement 818123 (iAtlantic) and by the Federal Ministry of Education and Research (BMBF) through the project METAscales (Grant No. 03F0955J), as well as the northern German states within the scope of the German Marine Research Alliance (DAM) mission mareXtreme. The authors gratefully acknowledge the Earth System Modelling Project (ESM) for funding this work by providing computing time on the ESM partition of the supercomputer JUWELS at the Juelich Supercomputing center (JSC).

https://doi.org/10.5194/egusphere-2025-571
Preprint. Discussion started: 17 February 2025

References

Amaya, D. J., Jacox, M. G., Alexander, M. A., Scott, J. D., Deser, C., Capotondi, A., and Phillips, A. S.: Bottom marine heatwaves along the continental shelves of North America, Nature Communications, 14, 1038, https://doi.org/10.1038/s41467-023-36567-0, 2023a.

Amaya, D. J., Jacox, M. G., Fewings, M. R., Saba, V. S., Stuecker, M. F., Rykaczewski, R. R., Ross, A. C., Stock, C. A., Capotondi, A., Petrik, C. M., Bograd, S. J., Alexander, M. A., Cheng, W., Hermann, A. J., Kearney, K. A., and Powell, B. S.: Marine heatwaves need clear definitions so coastal communities can adapt, Nature, 616, 29–32, https://doi.org/10.1038/d41586-023-00924-2, 2023b.

Arístegui, J., Barton, E. D., Álvarez Salgado, X. A., Santos, A. M. P., Figueiras, F. G., Kifani, S., Hernández-León, S., Mason, E., Machú, E., and Demarcq, H.: Sub-regional ecosystem variability in the Canary Current upwelling, Progress in Oceanography, 83, 33–48, https://doi.org/10.1016/j.pocean.2009.07.031, 2009.

Barnier, B., Madec, G., Penduff, T., Molines, J.-M., Treguier, A.-M., Le Sommer, J., Beckmann, A., Biastoch, A., Böning, C., Dengg, J., Derval, C., Durand, E., Gulev, S., Remy, E., Talandier, C., Theetten, S., Maltrud, M., McClean, J., and Cuevas, B.: Impact of partial steps and momentum advection schemes in a global ocean circulation model at eddy-permitting resolution, Ocean Dynamics, 56, 543–567, https://doi.org/10.1007/s10236-006-0082-1, 2006.

Behrens, E., Fernandez, D., and Sutton, P.: Meridional Oceanic Heat Transport Influences Marine Heatwaves in the Tasman Sea on Interannual to Decadal Timescales, Frontiers in Marine Science, 6, https://doi.org/10.3389/fmars.2019.00228, 2019.

Berthou, S., Renshaw, R., Smyth, T., Tinker, J., Grist, J. P., Wihsgott, J. U., Jones, S., Inall, M., Nolan, G., Berx, B., Arnold, A., Blunn, L. P., Castillo, J. M., Cotterill, D., Daly, E., Dow, G., Gómez, B., Fraser-Leonhardt, V., Hirschi, J. J.-M., Lewis, H. W., Mahmood, S., and Worsfold, M.: Exceptional atmospheric conditions in June 2023 generated a northwest European marine heatwave which contributed to breaking land temperature records, Communications Earth & Environment, 5, 287, https://doi.org/10.1038/s43247-024-01413-8, 2024.

Biastoch, A., Schwarzkopf, F. U., Getzlaff, K., Rühs, S., Martin, T., Scheinert, M., Schulzki, T., Handmann, P., Hummels, R., and Böning, C. W.: Regional imprints of changes in the Atlantic Meridional Overturning Circulation in the eddy-rich ocean model VIKING20X, Ocean Sci., 17, 1177–1211, https://doi.org/10.5194/os-17-1177-2021, publisher: Copernicus Publications, 2021.

Böning, C. W., Wagner, P., Handmann, P., Schwarzkopf, F. U., Getzlaff, K., and Biastoch, A.: Decadal changes in Atlantic overturning due to the excessive 1990s Labrador Sea convection, Nature Communications, 14, 4635, https://doi.org/10.1038/s41467-023-40323-9, 2023.

Chen, K., Gawarkiewicz, G., and Yang, J.: Mesoscale and Submesoscale Shelf-Ocean Exchanges Initialize an Advective Marine Heatwave, Journal of Geophysical Research: Oceans, 127, e2021JC017 927, https://doi.org/10.1029/2021JC017927, publisher: John Wiley & Sons, Ltd, 2022.

Chiswell, S. M.: Global Trends in Marine Heatwaves and Cold Spells: The Impacts of Fixed Versus Changing Baselines, Journal of Geophysical Research: Oceans, 127, e2022JC018 757, https://doi.org/10.1029/2022JC018757, publisher: John Wiley & Sons, Ltd, 2022.

Cropper, T. E., Hanna, E., and Bigg, G. R.: Spatial and temporal seasonal trends in coastal upwelling off Northwest Africa, 1981–2012, Deep Sea Research Part I: Oceanographic Research Papers, 86, 94–111, https://doi.org/10.1016/j.dsr.2014.01.007, 2014.

Debreu, L., Vouland, C., and Blayo, E.: AGRIF: Adaptive grid refinement in Fortran, Computers & Geosciences, 34, 8–13, https://doi.org/10.1016/j.cageo.2007.01.009, 2008.

Elzahaby, Y. and Schaeffer, A.: Observational Insight Into the Subsurface Anomalies of Marine Heatwaves, Frontiers in Marine Science, 6, https://doi.org/10.3389/fmars.2019.00745, 2019.

https://doi.org/10.5194/egusphere-2025-571
Preprint. Discussion started: 17 February 2025

Elzahaby, Y., Schaeffer, A., Roughan, M., and Delaux, S.: Oceanic Circulation Drives the Deepest and Longest Marine Heatwaves in the East Australian Current System, Geophysical Research Letters, 48, e2021GL094 785, https://doi.org/10.1029/2021GL094785, publisher: John Wiley & Sons, Ltd, 2021.

Fox, A. D., Handmann, P., Schmidt, C., Fraser, N., Rühs, S., Sanchez-Franks, A., Martin, T., Oltmanns, M., Johnson, C., Rath, W., Holliday, N. P., Biastoch, A., Cunningham, S. A., and Yashayaev, I.: Exceptional freshening and cooling in the eastern subpolar North Atlantic caused by reduced Labrador Sea surface heat loss, Ocean Sci., 18, 1507–1533, https://doi.org/10.5194/os-18-1507-2022, publisher: Copernicus Publications, 2022.

Fragkopoulou, E., Sen Gupta, A., Costello, M. J., Wernberg, T., Araújo, M. B., Serrão, E. A., De Clerck, O., and Assis, J.: Marine biodiversity exposed to prolonged and intense subsurface heatwaves, Nature Climate Change, 13, 1114–1121, https://doi.org/10.1038/s41558-023-01790-6, 2023.

Gawarkiewicz, G., Chen, K., Forsyth, J., Bahr, F., Mercer, A. M., Ellertson, A., Fratantoni, P., Seim, H., Haines, S., and Han, L.: Characteristics of an Advective Marine Heatwave in the Middle Atlantic Bight in Early 2017, Frontiers in Marine Science, 6, https://www.frontiersin.org/journals/marine-science/articles/10.3389/fmars.2019.00712, 2019.

Gelderloos, R., Katsman, C. A., and Drijfhout, S. S.: Assessing the Roles of Three Eddy Types in Restratifying the Labrador Sea after Deep Convection, Journal of Physical Oceanography, 41, 2102–2119, https://doi.org/10.1175/JPO-D-11-054.1, place: Boston MA, USA Publisher: American Meteorological Society, 2011.

Goes, M., Dong, S., Foltz, G. R., Goni, G., Volkov, D. L., and Wainer, I.: Modulation of Western South Atlantic Marine Heatwaves by Meridional Ocean Heat Transport, Journal of Geophysical Research: Oceans, 129, e2023JC019 715, https://doi.org/10.1029/2023JC019715, publisher: John Wiley & Sons, Ltd, 2024.

Großelindemann, H., Ryan, S., Ummenhofer, C. C., Martin, T., and Biastoch, A.: Marine Heatwaves and Their Depth Structures on the Northeast U.S. Continental Shelf, Frontiers in Climate, 4, 2022.

Guo, X., Gao, Y., Zhang, S., Wu, L., Chang, P., Cai, W., Zscheischler, J., Leung, L. R., Small, J., Danabasoglu, G., Thompson, L., and Gao, H.: Threat by marine heatwaves to adaptive large marine ecosystems in an eddy-resolving model, Nature Climate Change, 12, 179–186, https://doi.org/10.1038/s41558-021-01266-5, 2022.

Hobday, A. J., Alexander, L. V., Perkins, S. E., Smale, D. A., Straub, S. C., Oliver, E. C., Benthuysen, J. A., Burrows, M. T., Donat, M. G., Feng, M., Holbrook, N. J., Moore, P. J., Scannell, H. A., Sen Gupta, A., and Wernberg, T.: A hierarchical approach to defining marine heatwaves, Progress in Oceanography, 141, 227–238, https://doi.org/10.1016/j.pocean.2015.12.014, 2016.

Holbrook, N. J., Scannell, H. A., Sen Gupta, A., Benthuysen, J. A., Feng, M., Oliver, E. C. J., Alexander, L. V., Burrows, M. T., Donat, M. G., Hobday, A. J., Moore, P. J., Perkins-Kirkpatrick, S. E., Smale, D. A., Straub, S. C., and Wernberg, T.: A global assessment of marine heatwaves and their drivers, Nature Communications, 10, 2624, https://doi.org/10.1038/s41467-019-10206-z, 2019.

Hoving, H. J. T., Neitzel, P., Hauss, H., Christiansen, S., Kiko, R., Robison, B. H., Silva, P., and Körtzinger, A.: In situ observations show vertical community structure of pelagic fauna in the eastern tropical North Atlantic off Cape Verde, Scientific Reports, 10, 21 798, https://doi.org/10.1038/s41598-020-78255-9, 2020.

Huang, B., Liu, C., Banzon, V., Freeman, E., Graham, G., Hankins, B., Smith, T., and Zhang, H.-M.: Improvements of the Daily Optimum Interpolation Sea Surface Temperature (DOISST) Version 2.1, Journal of Climate, 34, 2923–2939, https://doi.org/10.1175/JCLI-D-20-0166.1, place: Boston MA, USA Publisher: American Meteorological Society, 2021.

Hövel, L., Brune, S., and Baehr, J.: Decadal Prediction of Marine Heatwaves in MPI-ESM, Geophysical Research Letters, 49, e2022GL099 347, https://doi.org/10.1029/2022GL099347, publisher: John Wiley & Sons, Ltd, 2022.

https://doi.org/10.5194/egusphere-2025-571
Preprint. Discussion started: 17 February 2025

Janjić, T., McLaughlin, D., Cohn, S. E., and Verlaan, M.: Conservation of Mass and Preservation of Positivity with Ensemble-Type Kalman Filter Algorithms, Monthly Weather Review, 142, 755–773, https://doi.org/10.1175/MWR-D-13-00056.1, place: Boston MA, USA Publisher: American Meteorological Society, 2014.

Kaboth-Bahr, S., Bahr, A., Stepanek, C., Catunda, M. C. A., Karas, C., Ziegler, M., Garcia-Gallardo, A., and Grunert, P.: Mediterranean heat injection to the North Atlantic delayed the intensification of Northern Hemisphere glaciations, Communications Earth & Environment, 2, 158, https://doi.org/10.1038/s43247-021-00232-5, 2021.

Krüger, J., Kjellsson, J., Kedzierski, R. P., and Claus, M.: Connecting North Atlantic SST Variability to European Heat Events over the Past Decades, Tellus A: Dynamic Meteorology and Oceanography, https://doi.org/10.16993/tellusa.3235, 2023.

Liu, M. and Tanhua, T.: Water masses in the Atlantic Ocean: characteristics and distributions, Ocean Science, 17, 463–486, https://doi.org/10.5194/os-17-463-2021, 2021.

Locarnini, R. A., Mishonov, A. V., Antonov, J. I., Boyer, T. P., Garcia, H. E., Baranova, O. K., Zweng, M. M., Paver, C. R., Reagan, J. R., Johnson, D. R., Hamilton, M., Seidov, 1948, D., and Levitus, S.: World ocean atlas 2013. Volume 1, Temperature, https://doi.org/10.7289/V55X26VD, 2013.

Madec, G.: NEMO ocean engine, Note du P\^ole de mod{\'e}lisation, Institut Pierre-Simon Laplace (IPSL), France, No 27, ISSN No 1288-1619, 2016.

Maldonado, M., Aguilar, R., Bannister, R. J., Bell, J. J., Conway, K. W., Dayton, P. K., Díaz, C., Gutt, J., Kelly, M., Kenchington, E. L. R., Leys, S. P., Pomponi, S. A., Rapp, H. T., Rützler, K., Tendal, O. S., Vacelet, J., and Young, C. M.: Sponge Grounds as Key Marine Habitats: A Synthetic Review of Types, Structure, Functional Roles, and Conservation Concerns, in: Marine Animal Forests: The Ecology of Benthic Biodiversity Hotspots, edited by Rossi, S., Bramanti, L., Gori, A., and Orejas, C., pp. 145–183, Springer International Publishing, Cham, ISBN 978-3-319-21012-4, https://doi.org/10.1007/978-3-319-21012-4_24, 2017.

Marzinelli, E. M., Williams, S. B., Babcock, R. C., Barrett, N. S., Johnson, C. R., Jordan, A., Kendrick, G. A., Pizarro, O. R., Smale, D. A., and Steinberg, P. D.: Large-Scale Geographic Variation in Distribution and Abundance of Australian Deep-Water Kelp Forests, PLOS ONE, 10, e0118 390, https://doi.org/10.1371/journal.pone.0118390, publisher: Public Library of Science, 2015.

Morato, T., Gonzalez-Irusta, J.-M., Dominguez-Carrio, C., Wei, C.-L., Davies, A., Sweetman, A. K., Taranto, G. H., Beazley, L., Garcia-Alegre, A., Grehan, A., Laffargue, P., Murillo, F. J., Sacau, M., Vaz, S., Kenchington, E., Arnaud-Haond, S., Callery, O., Chimienti, G., Cordes, E., Egilsdottir, H., Freiwald, A., Gasbarro, R., Gutierrez-Zarate, C., Gianni, M., Gilkinson, K., Wareham Hayes, V. E., Hebbeln, D., Hedges, K., Henry, L.-A., Johnson, D., Koen-Alonso, M., Lirette, C., Mastrototaro, F., Menot, L., Molodtsova, T., Duran Munoz, P., Orejas, C., Pennino, M. G., Puerta, P., Ragnarsson, S. A., Ramiro-Sanchez, B., Rice, J., Rivera, J., Roberts, J. M., Ross, S. W., Rueda, J. L., Sampaio, I., Snelgrove, P., Stirling, D., Treble, M. A., Urra, J., Vad, J., van Oevelen, D., Watling, L., Walkusz, W., Wienberg, C., Woillez, M., Levin, L. A., and Carreiro-Silva, M.: Climate-induced changes in the suitable habitat of cold-water corals and commercially important deep-sea fishes in the North Atlantic, Global Change Biology, 26, 2181–2202, https://doi.org/10.1111/gcb.14996, publisher: John Wiley & Sons, Ltd, 2020.

Oliver, E. C., Benthuysen, J. A., Darmaraki, S., Donat, M. G., Hobday, A. J., Holbrook, N. J., Schlegel, R. W., and Sen Gupta, A.: Marine Heatwaves, Annual Review of Marine Science, 13, 313–342, https://doi.org/https://doi.org/10.1146/annurev-marine-032720-095144, publisher: Annual Reviews Type: Journal Article, 2021.

Oliver, E. C. J., Donat, M. G., Burrows, M. T., Moore, P. J., Smale, D. A., Alexander, L. V., Benthuysen, J. A., Feng, M., Sen Gupta, A., Hobday, A. J., Holbrook, N. J., Perkins-Kirkpatrick, S. E., Scannell, H. A., Straub, S. C., and Wernberg, T.: Longer and more frequent marine heatwaves over the past century, Nature Communications, 9, 1324, https://doi.org/10.1038/s41467-018-03732-9, 2018.

https://doi.org/10.5194/egusphere-2025-571
Preprint. Discussion started: 17 February 2025

Petrelli, P.: XMHW: Xarray based code to identify Marine HeatWave events and their characteristics, https://doi.org/10.5281/zenodo.7668235, 2023.

Pilo, G. S., Holbrook, N. J., Kiss, A. E., and Hogg, A. M.: Sensitivity of Marine Heatwave Metrics to Ocean Model Resolution, Geophysical Research Letters, 46, 14 604–14 612, https://doi.org/10.1029/2019GL084928, publisher: John Wiley & Sons, Ltd, 2019.

Qiu, Z., Qiao, F., Jang, C. J., Zhang, L., and Song, Z.: Evaluation and projection of global marine heatwaves based on CMIP6 models, Deep Sea Research Part II: Topical Studies in Oceanography, 194, 104 998, https://doi.org/10.1016/j.dsr2.2021.104998, 2021.

Radfar, S., Moftakhari, H., and Moradkhani, H.: Rapid intensification of tropical cyclones in the Gulf of Mexico is more likely during marine heatwaves, Communications Earth & Environment, 5, 421, https://doi.org/10.1038/s43247-024-01578-2, 2024.

Rieck, J. K., Böning, C. W., and Getzlaff, K.: The Nature of Eddy Kinetic Energy in the Labrador Sea: Different Types of Mesoscale Eddies, Their Temporal Variability, and Impact on Deep Convection, J. Phys. Oceanogr., 49, 2075–2094, https://doi.org/10.1175/JPO-D-18-0243.1, 2019.

Roberts, J. M., Wheeler, A. J., and Freiwald, A.: Reefs of the Deep: The Biology and Geology of Cold-Water Coral Ecosystems, Science, 312, 543–547, https://doi.org/10.1126/science.1119861, publisher: American Association for the Advancement of Science, 2006.

Rühs, S., Oliver, E. C. J., Biastoch, A., Böning, C. W., Dowd, M., Getzlaff, K., Martin, T., and Myers, P. G.: Changing Spatial Patterns of Deep Convection in the Subpolar North Atlantic, Journal of Geophysical Research: Oceans, 126, e2021JC017 245, https://doi.org/10.1029/2021JC017245, publisher: John Wiley & Sons, Ltd, 2021.

Scannell, H. A., Johnson, G. C., Thompson, L., Lyman, J. M., and Riser, S. C.: Subsurface Evolution and Persistence of Marine Heatwaves in the Northeast Pacific, Geophysical Research Letters, 47, e2020GL090 548, https://doi.org/10.1029/2020GL090548, publisher: John Wiley & Sons, Ltd, 2020.

Schaeffer, A. and Roughan, M.: Subsurface intensification of marine heatwaves off southeastern Australia: The role of stratification and local winds, Geophysical Research Letters, 44, 5025–5033, https://doi.org/10.1002/2017GL073714, publisher: John Wiley & Sons, Ltd, 2017.

Schulzki, T., Henry, L.-A., Roberts, J. M., Rakka, M., Ross, S. W., and Biastoch, A.: Mesoscale ocean eddies determine dispersal and connectivity of corals at the RMS Titanic wreck site, Deep Sea Research Part I: Oceanographic Research Papers, 213, 104 404, https://doi.org/10.1016/j.dsr.2024.104404, 2024.

Schulzki, T., Schwarzkopf, F. U., and Biastoch, A.: Atlantic wide detection of marine heatwaves beyond the surface in a high-resolution model [dataset], GEOMAR Helmholtz Centre for Ocean Research Kiel [distributor], https://hdl.handle.net/20.500.12085/49913d6b-4c70-43cb-9d3c-b4b73b0b8291, 2025a.

Schulzki, T., Schwarzkopf, F. U., and Biastoch, A.: An Atlantic wide assessment of marine heatwaves beyond thesurface in an eddy-rich ocean model [dataset], GEOMAR Helmholtz Centre for Ocean Research Kiel [distributor], https://hdl.handle.net/20.500.12085/a3279a60-e9ef-437f-bd34-c3e156181e98, 2025b.

Short, J., Foster, T., Falter, J., Kendrick, G. A., and McCulloch, M. T.: Crustose coralline algal growth, calcification and mortality following a marine heatwave in Western Australia, Continental Shelf Research, 106, 38–44, https://doi.org/10.1016/j.csr.2015.07.003, 2015.

Smale, D. A., Wernberg, T., Oliver, E. C. J., Thomsen, M., Harvey, B. P., Straub, S. C., Burrows, M. T., Alexander, L. V., Benthuysen, J. A., Donat, M. G., Feng, M., Hobday, A. J., Holbrook, N. J., Perkins-Kirkpatrick, S. E., Scannell, H. A., Sen Gupta, A., Payne, B. L., and Moore, P. J.: Marine heatwaves threaten global biodiversity and the provision of ecosystem services, Nature Climate Change, 9, 306–312, https://doi.org/10.1038/s41558-019-0412-1, 2019.

https://doi.org/10.5194/egusphere-2025-571
Preprint. Discussion started: 17 February 2025

Smith, K. E., Burrows, M. T., Hobday, A. J., King, N. G., Moore, P. J., Sen Gupta, A., Thomsen, M. S., Wernberg, T., and Smale, D. A.: Biological Impacts of Marine Heatwaves, Annual Review of Marine Science, 15, 119–145, https://doi.org/https://doi.org/10.1146/annurev-marine-032122-121437, 2023.

Stenvers, V. I., Hauss, H., Osborn, K. J., Neitzel, P., Merten, V., Scheer, S., Robison, B. H., Freitas, R., and Hoving, H. J. T.: Distribution, associations and role in the biological carbon pump of Pyrosoma atlanticum (Tunicata, Thaliacea) off Cabo Verde, NE Atlantic, Scientific Reports, 11, 9231, https://doi.org/10.1038/s41598-021-88208-5, 2021.

Sun, D., Li, F., Jing, Z., Hu, S., and Zhang, B.: Frequent marine heatwaves hidden below the surface of the global ocean, Nature Geoscience, 16, 1099–1104, https://doi.org/10.1038/s41561-023-01325-w, 2023.

Tsujino, H., Urakawa, S., Nakano, H., Small, R. J., Kim, W. M., Yeager, S. G., Danabasoglu, G., Suzuki, T., Bamber, J. L., Bentsen, M., Böning, C. W., Bozec, A., Chassignet, E. P., Curchitser, E., Boeira Dias, F., Durack, P. J., Griffies, S. M., Harada, Y., Ilicak, M., Josey, S. A., Kobayashi, C., Kobayashi, S., Komuro, Y., Large, W. G., Le Sommer, J., Marsland, S. J., Masina, S., Scheinert, M., Tomita, H., Valdivieso, M., and Yamazaki, D.: JRA-55 based surface dataset for driving ocean–sea-ice models (JRA55-do), Ocean Modelling, 130, 79–139, https://doi.org/10.1016/j.ocemod.2018.07.002, 2018.

Tsujino, H., Urakawa, L. S., Griffies, S. M., Danabasoglu, G., Adcroft, A. J., Amaral, A. E., Arsouze, T., Bentsen, M., Bernardello, R., Böning, C. W., Bozec, A., Chassignet, E. P., Danilov, S., Dussin, R., Exarchou, E., Fogli, P. G., Fox-Kemper, B., Guo, C., Ilicak, M., Iovino, D., Kim, W. M., Koldunov, N., Lapin, V., Li, Y., Lin, P., Lindsay, K., Liu, H., Long, M. C., Komuro, Y., Marsland, S. J., Masina, S., Nummelin, A., Rieck, J. K., Ruprich-Robert, Y., Scheinert, M., Sicardi, V., Sidorenko, D., Suzuki, T., Tatebe, H., Wang, Q., Yeager, S. G., and Yu, Z.: Evaluation of global ocean–sea-ice model simulations based on the experimental protocols of the Ocean Model Intercomparison Project phase 2 (OMIP-2), Geosci. Model Dev., 13, 3643–3708, https://doi.org/10.5194/gmd-13-3643-2020, publisher: Copernicus Publications, 2020.

Vinha, B., Murillo, F. J., Schumacher, M., Hansteen, T. H., Schwarzkopf, F. U., Biastoch, A., Kenchington, E., Piraino, S., Orejas, C., and Huvenne, V. A. I.: Ensemble modelling to predict the distribution of vulnerable marine ecosystems indicator taxa on data-limited seamounts of Cabo Verde (NW Africa), Diversity and Distributions, 30, e13 896, https://doi.org/10.1111/ddi.13896, publisher: John Wiley & Sons, Ltd, 2024.

WMO-No.1203: WMO Guidelines on the Calculation of Climate Normals, https://community.wmo.int/en/wmo-climatological-normals, 2017.

Wu, T. and He, R.: Gulf Stream mesoscale variabilities drive bottom marine heatwaves in Northwest Atlantic continental margin methane seeps, Communications Earth & Environment, 5, 574, https://doi.org/10.1038/s43247-024-01742-8, 2024.

Wyatt, A. S. J., Leichter, J. J., Washburn, L., Kui, L., Edmunds, P. J., and Burgess, S. C.: Hidden heatwaves and severe coral bleaching linked to mesoscale eddies and thermocline dynamics, Nature Communications, 14, 25, https://doi.org/10.1038/s41467-022-35550-5, 2023.

Xu, T., Newman, M., Capotondi, A., Stevenson, S., Di Lorenzo, E., and Alexander, M. A.: An increase in marine heatwaves without significant changes in surface ocean temperature variability, Nature Communications, 13, 7396, https://doi.org/10.1038/s41467-022-34934-x, 2022.

Zeng, Y. and Janjić, T.: Study of conservation laws with the Local Ensemble Transform Kalman Filter, Quarterly Journal of the Royal Meteorological Society, 142, 2359–2372, https://doi.org/10.1002/qj.2829, publisher: John Wiley & Sons, Ltd, 2016.

Zhang, Y., Du, Y., Feng, M., and Hobday, A. J.: Vertical structures of marine heatwaves, Nature Communications, 14, 6483, https://doi.org/10.1038/s41467-023-42219-0, 2023.

https://doi.org/10.5194/egusphere-2025-571
Preprint. Discussion started: 17 February 2025

Zweng, M. M., Reagan, J. R., Antonov, J. I., Locarnini, R. A., Mishonov, A. V., Boyer, T. P., Garcia, H. E., Baranova, O. K., Johnson, D. R., Seidov, 1948, D., Biddle, M. M., and Levitus, S.: World ocean atlas 2013. Volume 2, Salinity, https://doi.org/10.7289/V5251G4D, 2013.